

ผลของตัวเร่งปฏิกิริยาชนิดซัลฟิनाไมด์ สารก่อโคม และกราฟีนต่อการเกิดและสมบัติของโคมยาง  
ธรรมชาติ



บทคัดย่อและแฟ้มข้อมูลฉบับเต็มของวิทยานิพนธ์ตั้งแต่ปีการศึกษา 2554 ที่ให้บริการในคลังปัญญาจุฬาฯ (CUIR)  
เป็นแฟ้มข้อมูลของนิสิตเจ้าของวิทยานิพนธ์ ที่ส่งผ่านทางบัณฑิตวิทยาลัย

The abstract and full text of theses from the academic year 2011 in Chulalongkorn University Intellectual Repository (CUIR)  
are the thesis authors' files submitted through the University Graduate School.

วิทยานิพนธ์นี้เป็นส่วนหนึ่งของการศึกษาตามหลักสูตรปริญญาวิทยาศาสตรดุษฎีบัณฑิต  
สาขาวิชาวิศวกรรมเคมี ภาควิชาวิศวกรรมเคมี  
คณะวิศวกรรมศาสตร์ จุฬาลงกรณ์มหาวิทยาลัย  
ปีการศึกษา 2558  
ลิขสิทธิ์ของจุฬาลงกรณ์มหาวิทยาลัย

EFFECT OF SULFENAMIDE ACCELERATORS, CHEMICAL BLOWING AGENT AND GRAPHENE  
ON FORMATION AND PROPERTIES OF NATURAL RUBBER FOAM

Mr. Pollawat Jaroenthonkajonchai



A Dissertation Submitted in Partial Fulfillment of the Requirements  
for the Degree of Doctor of Engineering Program in Chemical Engineering

Department of Chemical Engineering

Faculty of Engineering

Chulalongkorn University

Academic Year 2015

Copyright of Chulalongkorn University

Thesis Title	EFFECT OF SULFENAMIDE ACCELERATORS, CHEMICAL BLOWING AGENT AND GRAPHENE ON FORMATION AND PROPERTIES OF NATURAL RUBBER FOAM
By	Mr. Pollawat Jaroenthonkajonchai
Field of Study	Chemical Engineering
Thesis Advisor	Associate Professor Anongnat Somwangthanaroj, Ph.D.

---

Accepted by the Faculty of Engineering, Chulalongkorn University in Partial  
Fulfillment of the Requirements for the Doctoral Degree

.....Dean of the Faculty of Engineering  
(Associate Professor Supot Teachavorasinskun, D.Eng.)

THESIS COMMITTEE

.....Chairman  
(Associate Professor Artiwan Shotipruk, Ph.D.)

.....Thesis Advisor  
(Associate Professor Anongnat Somwangthanaroj, Ph.D.)

.....Examiner  
(Assistant Professor Kanoktip Boonkerd, Ph.D.)

.....Examiner  
(Associate Professor Siriporn Damrongsakkul, Ph.D.)

.....External Examiner  
(Assistant Professor Wanchai Lerdwijitjarud, Ph.D.)

พลวัฒน์ เจริญธรรมจรชัย : ผลของตัวเร่งปฏิกิริยาชนิดซัลฟิनाไมด์ สารก่อโฟม และกราฟีนต่อการเกิดและสมบัติของโฟมยางธรรมชาติ (EFFECT OF SULFENAMIDE ACCELERATORS, CHEMICAL BLOWING AGENT AND GRAPHENE ON FORMATION AND PROPERTIES OF NATURAL RUBBER FOAM) อ.ที่ปรึกษาวิทยานิพนธ์หลัก: รศ. ดร. อนงค์นาฏ สมหวังธนโรจน์, 120 หน้า.

การผลิตโฟมยางธรรมชาติด้วยวิธีการใช้สารก่อโฟมด้วยกระบวนการกดอัดในแม่พิมพ์พบว่ายังมีปัญหาเรื่องการขยายตัวของชิ้นงานเมื่อนำชิ้นงานออกจากแม่พิมพ์ งานวิจัยนี้ได้ศึกษาผลของปริมาณสารก่อโฟม โครงสร้างของตัวเร่งปฏิกิริยาชนิดซัลฟิनाไมด์ และผลของการเติมกราฟีนที่ปรับปรุงพื้นผิวด้วยไซโคลเฮกซิลไดเอมีนผ่านปฏิกิริยาของไดอะโซเนียมเพื่อแก้ไขปัญหาดังกล่าวและพัฒนาสมบัติของโฟมยางธรรมชาติ แม้ว่าปริมาณสารก่อโฟมที่เพิ่มขึ้นจะช่วยเร่งปฏิกิริยาการเชื่อมขวางโมเลกุลของยางธรรมชาติด้วยกำมะถันเนื่องจากสารประกอบเอมีนที่ได้จากการสลายตัวทางความร้อนของสารก่อโฟม แต่ปริมาณสารก่อโฟมที่เพิ่มขึ้นทำให้ค่าอันดับการเกิดปฏิกิริยาของปฏิกิริยาการเชื่อมขวางโมเลกุลของยางลดลง โฟมยางธรรมชาติที่มีส่วนผสมของสารก่อโฟม 4 ส่วนในร้อยละของยางให้พองก๊าซที่มีขนาดเล็กและสมบัติที่ดี สำหรับผลกระทบของโครงสร้างของตัวเร่งปฏิกิริยาชนิดซัลฟิनाไมด์พบว่าโฟมยางธรรมชาติที่ใช้ตัวเร่งปฏิกิริยาไซโคลเฮกซิลเบนโซไทโออาโซล-2-ซัลฟิनाไมด์ช่วยเร่งปฏิกิริยาการเชื่อมขวางโมเลกุลของยางด้วยกำมะถันได้เร็วที่สุด ส่งผลให้มีพองก๊าซขนาดเล็ก มีช่วงการกระจายตัวของขนาดพองก๊าซที่แคบและสัมประสิทธิ์การขยายตัวทางความร้อนต่ำ นอกจากนี้โฟมยางธรรมชาติที่ใช้ตัวเร่งปฏิกิริยาดังกล่าวยังมีค่าพลังงานกระตุ้นต่ำที่สุด เนื่องจากมีสถานะความเป็นเบสสูงจากความเสถียรของเอมีนหลังจากตัวเร่งปฏิกิริยาแตกตัวและสร้างเป็นสารประกอบเชิงซ้อนกับสารเคมีในระบบการเชื่อมขวางโมเลกุลของยางด้วยกำมะถัน ปัจจัยสุดท้ายคือผลของปริมาณกราฟีนและการปรับปรุงสภาพพื้นผิวของกราฟีน พบว่าปริมาณกราฟีนที่เพิ่มมากขึ้นจะช่วยเร่งปฏิกิริยาการเชื่อมขวางโมเลกุลของยางด้วยกำมะถัน เนื่องจากผลของหมู่ออกซิเจนที่ยังเหลืออยู่บนพื้นผิวของกราฟีน นอกจากนี้พบว่ากราฟีนสามารถกระจายตัวได้ดีในยางเมื่อทำการปรับสภาพพื้นผิว แต่ปฏิกิริยาการเชื่อมขวางโมเลกุลของยางด้วยกำมะถันเกิดช้าที่สุด เนื่องจากปฏิกิริยาของหมู่เอมีนบนไซโคลเฮกซิลไดเอมีนกับหมู่ออกซิเจนที่อยู่บนพื้นผิวของกราฟีน และพบว่าสูตรโฟมยางธรรมชาติที่ใส่กราฟีนที่ทำการปรับสภาพพื้นผิวที่ 3 ส่วนในร้อยละของยางให้ค่าทนแรงดึงที่สูงที่สุด เนื่องจากการกระจายตัวของอนุภาคกราฟีนที่ดีและค่าความหนาแน่นของพองก๊าซที่ต่ำ

ภาควิชา วิศวกรรมเคมี ลายมือชื่อนิสิต .....

สาขาวิชา วิศวกรรมเคมี ลายมือชื่อ อ.ที่ปรึกษาหลัก .....

ปีการศึกษา 2558

# # 5571447421 : MAJOR CHEMICAL ENGINEERING

KEYWORDS: NATURAL RUBBER FOAM (NRF) / CURE KINETICS / SULFENAMIDE / GRAPHENE / AZODICABONAMIDE

POLLAWAT JAROENTHONKAJONCHAI: EFFECT OF SULFENAMIDE ACCELERATORS, CHEMICAL BLOWING AGENT AND GRAPHENE ON FORMATION AND PROPERTIES OF NATURAL RUBBER FOAM. ADVISOR: ASSOC. PROF. ANONGNAT SOMWANGTHANAROJ, Ph.D., 120 pp.

Natural rubber foam (NRF) was produced by chemical blowing technique with compression molding process. This process still has a problem with oversized dimension after removing specimen from the mold. The effect of azodicarbonamide which is the chemical blowing agent, sulfenamide accelerators and surface treated graphene with cyclohexyl diamine via diazonium reaction were investigated to solve this problem and improve properties of NRF specimen. Although the presence of azodicarbonamide can accelerate sulfur vulcanization due to amine derivatives from thermal decomposition of chemical blowing agent, NRF with high content of azodicarbonamide reduces the m order of autocatalytic reaction which means low crosslink of rubber molecules. Moreover, NRF at 4 phr of azodicarbonamide shows the smallest bubble diameter with good properties. The different chemical structures of sulfenamide accelerators are also studied. NRF with N-cyclohexyl benzothiazole-2-sulfenamide (CBS) system reveals the fastest sulfur vulcanization rate resulting in the smallest bubble diameter with narrow size distribution and lowest thermal expansion coefficient. This system also has the lowest activation energy ( $E_a$ ) among other rubber foams with sulfenamide accelerators owing to high basicity from high stability of amine species after this accelerator forms as a complex species with other ingredients in sulfur vulcanization system. The last factor that should be concerned is the presence of graphene and surface treated graphene with cyclohexyl diamine via diazonium reaction. The higher graphene content in rubber matrix, the faster sulfur vulcanization rate is obtained as a result of the remaining oxygen functional group on surface of graphene. Furthermore, surface treatment of graphene improved dispersion in rubber matrix. It also shows the slowest sulfur vulcanization rate due to the reaction between cyclohexyl diamine and oxygen functional groups on the graphene surface. NRF with 3 phr of treated graphene has the highest tensile strength at break due to good dispersion of graphene particle and low cell density in natural rubber foam product.

Department: Chemical Engineering

Student's Signature .....

Field of Study: Chemical Engineering

Advisor's Signature .....

Academic Year: 2015

## ACKNOWLEDGEMENTS

I would like to acknowledge the 90th Anniversary of Chulalongkorn University Scholarship (Ratchadaphiseksomphot Endowment Fund) and the Royal Golden Jubilee Ph.D. Scholarship (PHD/0264/2553) by Thailand Research Fund for financial support. I would like to thank Dr. Kanet Wongravee from Faculty of Science, Chulalongkorn University for useful suggestion and Sunny World Chemical Co., Ltd., Behn Mayer Co., Ltd., as well as AF Goodrich chemical Co., Ltd., Thailand for providing chemicals in this research.



## CONTENTS

	Page
THAI ABSTRACT .....	iv
ENGLISH ABSTRACT .....	v
ACKNOWLEDGEMENTS .....	vi
CONTENTS .....	vii
CHAPTER I INTRODUCTION.....	1
1.1. General Introduction .....	1
1.2. Objectives of the research.....	2
1.3. Scopes of the research.....	2
CHAPTER II THEORY AND LITERATURE REVIEWS .....	4
2.1. Natural rubber foam process .....	4
2.2. Sulfur vulcanization reaction.....	6
2.3. Thermal decomposition of chemical blowing agent .....	10
2.4. Effect of filler on sulfur vulcanization.....	11
2.5. Cure kinetics and kinetic parameters of natural rubber .....	15
2.6. Parameters that affect properties of natural rubber foam .....	19
CHAPTER III EXPERIMENTS.....	21
3.1. Materials .....	22
3.2. Sample preparation.....	23
3.2.1. Surface treatment of graphene by cyclohexyl diamine via diazonium reaction.....	23
3.2.2. Natural rubber compounding process .....	24
3.2.3. Compression molding process of natural rubber foam .....	25
3.3. Characterizations.....	26

	Page
3.3.1. Mooney viscosity .....	26
3.3.2. Functional group analysis of graphene nanoplatelet.....	26
3.3.3. Cure characteristics .....	27
3.3.4. Solvent absorption and gel content during sulfur vulcanization reaction.....	28
3.3.5. Morphology.....	29
3.3.6. Cell density calculation .....	30
3.3.7. Tensile properties and compression set .....	31
3.3.8. Thermal properties .....	31
CHAPTER IV RESULTS AND DISCUSSION .....	34
4.1. Effect of azodicarbonamide content on cure characteristics and properties of natural rubber foam.....	34
4.1.1. Effect of azodicarbonamide content on cure kinetics and kinetic parameters of NRF product .....	34
4.1.2. Effect of azodicarbonamide content on morphology of NRF product.....	47
4.1.3. Effect of azodicarbonamide on physical and thermal properties of NRF product.....	49
4.2. Effect of sulfenamide accelerators on cure characteristics and properties of natural rubber foam.....	54
4.2.1. Effect of sulfenamide accelerators on cure kinetics and kinetic parameters of NRF product .....	54
4.2.2. Effect of sulfenamide accelerators on morphology of NRF product .....	62
4.2.3. Effect of sulfenamide accelerators on physical, mechanical and thermal properties of NRF product.....	63



4.3. Effect of graphene and surface treatment of graphene on cure characteristics and properties of natural rubber foam .....	69
4.3.1. Surface chemistry of graphene.....	69
4.3.2. Cure characteristics of NR/graphene nanocomposite foam.....	75
4.3.3. Morphology of graphene/natural rubber foam nanocomposites .....	78
4.3.4. Physical, mechanical and thermal properties of NR/graphene nanocomposite foam.....	81
CHAPTER V CONCLUSIONS AND RECOMMENDATION .....	87
REFERENCES .....	90
Appendix A Mooney viscosity of natural rubber.....	108
Appendix B Solvent absorption and gel content of vulcanized natural rubber ....	109
Appendix C Particle size distribution.....	110
Appendix D Stress-stain curve of NR/graphene nanocomposite foam.....	119
VITA.....	120

## LIST OF FIGURE

Figure 2.1 sulfur vulcanization reaction of natural rubber [11].....	5
Figure 2.2 Scorch delay mechanism of sulfenamide accelerators [18].....	8
Figure 2.3 The chemical structures of sulfenamide accelerators .....	9
Figure 3.1 The experimental flowchart of natural rubber foam.....	22
Figure 4.1 Torque measurements of vulcanized natural rubber and natural rubber foam when using MBS accelerator system with different chemical blowing agent contents at 155°C .....	37
Figure 4.2 Mechanism of sulfurating species of activator with CBS accelerator [65] ...	38
Figure 4.3 Cure characteristics of vulcanized natural rubber and natural rubber foam when using MBS accelerator with different chemical blowing agent contents at 155°C .....	39
Figure 4.4 The possible mechanism of thermal decomposition of azodicarbonamide [40-42] .....	40
Figure 4.5 Torque measurement of natural rubber foam when using MBS accelerator at 3 phr of chemical blowing agent with various processing temperatures .....	41
Figure 4.6 Cure characteristics of natural rubber foam when using MBS accelerator at 3 phr of chemical blowing agent with various processing temperatures .....	42
Figure 4.7 The linear plot of $\ln K(T)$ vs $1/T$ of vulcanized natural rubber and natural rubber foam when using MBS accelerator with different chemical blowing agent contents .....	43
Figure 4.8 SEM images of natural rubber foam specimen produced at 155°C of processing temperature (a) NRF-MBS-B3, (b) NRF-MBS-B4, (c) NRF-MBS-B5, (d) NRF-MBS-B6 .....	49

Figure 4.9 Bulk densities of vulcanized natural rubber and natural rubber foam with different chemical blowing agent contents produced at 155°C of processing temperature.....	51
Figure 4.10 Volume expansion of natural rubber foam produced at 155°C of processing temperature compared to vulcanized natural rubber.....	52
Figure 4.11 Thermal expansion property of vulcanized natural rubber and natural rubber foam produced at 155°C of processing temperature with different chemical blowing agent contents.....	54
Figure 4.12 Torque measurement of natural rubber foam at 4 phr of chemical blowing agent produced at 155°C of processing temperature with different sulfenamide accelerators.....	57
Figure 4.13 Cure characteristics of natural rubber foam at 4 phr of chemical blowing agent produced at 155°C of processing temperature with different sulfenamide accelerators.....	58
Figure 4.14 Cure characteristics of natural rubber foam at 4 phr of chemical blowing agent with different sulfenamide accelerators and processing temperatures.....	59
Figure 4.15 SEM images of natural rubber foam specimen at 4 phr of chemical blowing agent produced at 155°C of processing temperature (a) NRF-MBS-B4, (b) NRF-TBBS-B4, (c) NRF-CBS-B4 and (d) NRF-CBS2-B4.....	63
Figure 4.16 Percentage of compression set of natural rubber foam at 4 phr of chemical blowing agent with different sulfenamide accelerators produced at 155°C of processing temperature.....	66
Figure 4.17 Thermal expansion coefficient of natural rubber foam at 4 phr of chemical blowing agent with different sulfenamide accelerators produced at 155°C of processing temperature.....	68

Figure 4.18 Thermal conductivity of natural rubber foam at 4 phr of chemical blowing agent with different sulfenamide accelerator produced at 155°C of processing temperature.....	69
Figure 4.19 FTIR spectrum of untreated graphene (UG) and treated surface of graphene by cyclohexyl diamine (CG).....	71
Figure 4.20 Raman spectrum of untreated graphene (UG) and treated surface of graphene by cyclohexyl diamine (CG).....	72
Figure 4.21 Thermal decomposition of untreated graphene (UG) and treated surface of graphene by cyclohexyl diamine (CG) .....	73
Figure 4.22 Possible mechanism of surface treatment of graphene by cyclohexyl diamine via diazonium reaction .....	74
Figure 4.23 Torque measurement of NRF at 155°C with untreated graphene (UG) and treated surface of graphene (CG).....	77
Figure 4.24 Cure characteristics of NRF at 155°C with untreated graphene (UG) and treated surface of graphene (CG) .....	77
Figure 4.25 TEM images of vulcanized natural rubber at 3 phr of untreated graphene (a) and treated surface of graphene with cyclohexyl diamine (b).....	79
Figure 4.26 SEM images of (a) NRF-CBS-B5, (b) NRF-CBS-B5-UG1, (c) NRF-CBS-B5-UG2, (d) NRF-CBS-B5-UG3, (d) NRF-CBS-B5-CG3.....	80

### LIST OF TABLE

Table 2.1 Characteristics of accelerator class in vulcanization system [7].....	7
Table 3.1 The chemical composition of rubber compound .....	25
Table 3.2 Measurement and characterization of sample .....	33
Table 4.1 Summary of the cure kinetics and kinetic parameters of vulcanized natural rubber and natural rubber foam when using MBS accelerator with different chemical blowing agent contents .....	44
Table 4.2 Summary of the cure kinetics and kinetic parameters of natural rubber foam at 4 phr of chemical blowing agent with different sulfenamide accelerators....	60
Table 4.3 Physical properties of NRF with different sulfenamide accelerators.....	65
Table 4.4 Physical properties of NRF with and without untreated graphene (UG) and surface treatment of graphene with cyclohexyl diamine (CG) .....	82
Table 4.5 Mechanical properties of NRF with and without untreated graphene (UG) and surface treatment of graphene with cyclohexyl diamine (CG) .....	84
Table 4.6 Thermal properties of NRF with and without untreated graphene (UG) and surface treatment of graphene with cyclohexyl diamine (CG) .....	86

## CHAPTER I

### INTRODUCTION

#### 1.1. General Introduction

Natural rubber foam (NRF) is used in many applications because of its light weight, thermal insulation and sound absorption. NRF could be produced in many methods such as mechanical whipping of gas, volatilization of low boiling point liquid, volatilization of gas from reaction, expansion of dissolved gas by reducing pressure, addition of hollow microsphere, expansion of gas-filled bead and decomposition of chemical blowing agent. In this research, it is produced by chemical blowing agent technique with compression molding process because this technique can be used to produce complexly shaped rubber foam specimen. However this process still has the major problem from oversized dimension of specimen when it is removed from the mold. In order to solve this issue, our research focuses on the balance of thermal decomposition reaction of chemical blowing agent and crosslink reaction of rubber molecules by sulfur. To understand these two reactions that occur at the same time during compression of natural rubber compound in the mold, the effects of azodicarbonamide content which is the chemical blowing agent, the chemical structure of sulfenamide accelerators, and

incorporation of graphene with and without surface treatment with cyclohexyl diamine via diazonium reaction on the properties of NRF product are investigated.

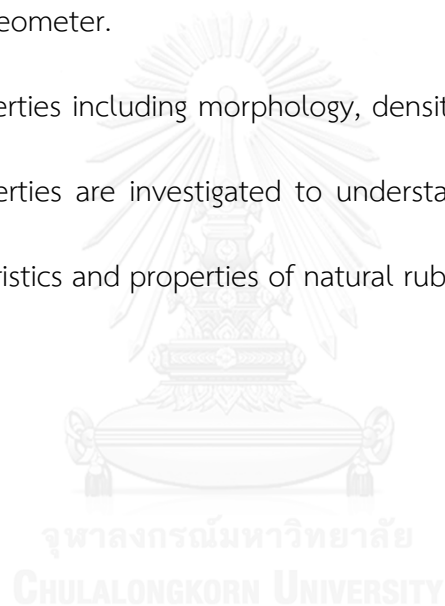
### 1.2. Objectives of the research

1. To study cure kinetics and kinetic parameters of natural rubber foam when the amount of chemical blowing agent, types of sulfenamide accelerators and amount of graphene with and without surface treatment by cyclohexyl diamine are varied
2. To investigate the effects of chemical blowing agent, structure of sulfenamide accelerators and surface treatment of graphene by cyclohexyl diamine on properties of natural rubber foam
3. To understand how to control the final dimension of natural rubber foam specimen

### 1.3. Scopes of the research

1. Natural rubber foam is prepared by using internal mixer and compression molding process with chemical blowing agent technique.
2. The chemical blowing agent, which is azodicarbonamide, is varied in the range of 0-6 phr.
3. Sulfenamide accelerators: N-cyclohexyl benzothiazole-2-sulfenamide (CBS), N-t-butylbenzothiazole-2-sulfenamide (TBBS) and 2-morpholinothiobenzotiazole (MBS) are used in this research.

4. The amount of graphene content is varied in the range of 0-3 phr and the effect of surface treatment of graphene by cyclohexyl diamine is studied at 3 phr of graphene content.
5. Surface treatment of graphene is characterized by FTIR, Raman spectroscopy and thermal degradation techniques.
6. Cure kinetics and kinetic parameters are calculated from rheograph from moving die rheometer.
7. Physical properties including morphology, density, as well as mechanical and thermal properties are investigated to understand the relationship between cure characteristics and properties of natural rubber foam (NRF) product.





## CHAPTER II

### THEORY AND LITERATURE REVIEWS

#### 2.1. Natural rubber foam process

Rubber foam is used in many applications due to its excellent properties such as insulation, light weight, as well as energy and sound absorption [1-4]. There are several methods to produce foam or cellular structure of rubber such as mechanical whipping of gas, volatilization of low boiling point liquid, volatilization of gas from reaction, expansion of dissolved gas by reducing pressure, addition of hollow microsphere, expansion of gas-filled bead and decomposition of chemical blowing agent [2]. The chemical blowing agent technique is used in this research because this technique is suitable for fabricating the complex shape of natural rubber foam (NRF) specimen by compression molding process. For this technique, during thermal decomposition of chemical blowing agent to produce gas, rubber chain is linked together to form 3-dimensional network by crosslink agent, forming sponge rubber. There are many techniques to crosslink polymer chain depending on characteristics of rubber and application in industries. The most popular techniques are using sulfur vulcanization and peroxide reaction [1, 5-7] Although using peroxide as a crosslink agent could solve the blooming of crosslink agent on the specimen's surface, the high price and difficulty of controllable reaction during crosslink of rubber molecules

by peroxide could be encountered [7]. In this research, crosslink reaction of rubber molecules with sulfur is selected because the sulfur vulcanization rate is not too fast to control the crosslink reaction and this system with sulfenamide accelerators shows the scorch delay mechanism which is the useful mechanism for preventing crosslink reaction during mixing rubber in an internal mixer. The rubber chain is linked with sulfur molecule by sulfur vulcanizing agent during compression molding process [1, 3, 7-10]. The common mechanism of crosslink reaction with sulfur is shown in Figure 2.1 [11].

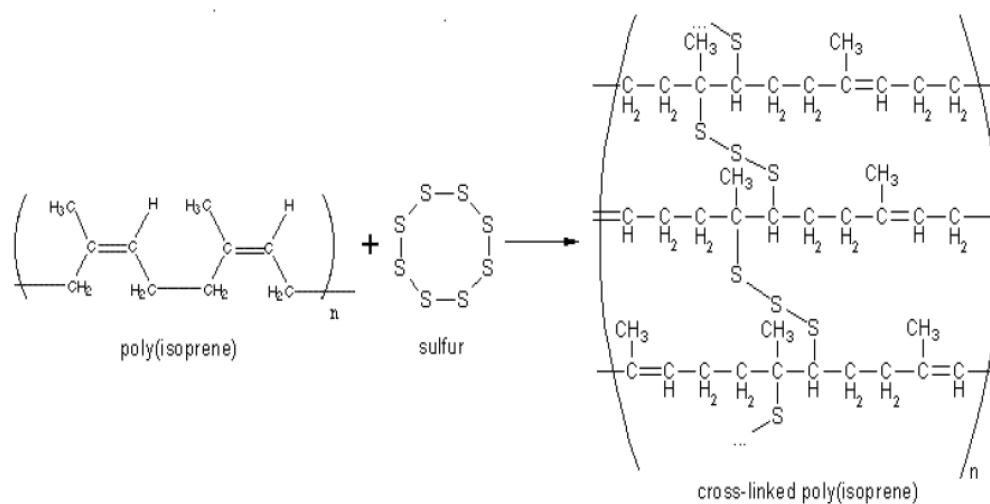


Figure 2.1 sulfur vulcanization reaction of natural rubber [11]

## 2.2. Sulfur vulcanization reaction

In sulfur vulcanization system, sulfur and heat are not enough to produce the strong 3-D network of rubber molecules; some chemicals have to be added to the system for accelerating and increasing reaction efficiency. The activator used for increasing vulcanization efficiency is zinc oxide (ZnO) and the substance for increasing wet ability of organic and inorganic substances in rubber compound is steric acid. It works together with ZnO and other chemicals to form activated complex [3]. Moreover, the accelerator is one of the most important factors to accelerate sulfur vulcanization or crosslink time of natural rubber molecules [3, 7]. There are many accelerators that can be used in sulfur vulcanization [7, 12-19]. The primary group of accelerator is comprised of thiazoles, sulfenamide and sulfenimide. Another group of accelerator which is called secondary accelerator includes guanidines, thiurams, dithiocarbamates and dithiophosphates. Generally, the secondary accelerator is used as co-accelerator with the primary accelerator to increase the rate of sulfur vulcanization [20-28]. Due to the different chemical structures of accelerators, the different response speed and chemical mechanism are obtained. The example of response speed of some accelerators is displayed as follow [7, 29].

Table 2.1 Characteristics of accelerator class in vulcanization system [7]

Class	Response speed	Commercial name
Guanidines	Medium	DPG, DOTG
Thiazoles	Semi-fast	MBT, MBTS
Sulfenamides	Fast, delayed action	CBS, TBBS, MBS, DCBS
Dithiophosphates	Fast	ZBPD
Thiurams	Very fast	TMTD, TMTM, TETD
Dithiocarbamates	Very fast	ZDMC, ZDBC

The sulfenamide accelerators are chosen in this research because of its fast acceleration rate with delayed scorch response. The scorch time is the time that accelerator and activator form complex structure before the crosslink chemistry occurs. Scorch delay mechanism is useful in our research because the rubber compound is mixed with all chemicals in an internal mixer in one step that differs from the common method in industries. In rubber foam manufacturing process, the rubber compound is separated into two-step mixing. The first step is to mix all the chemicals except chemical blowing agent and sulfur in banbury or internal mixer to prevent the crosslink reaction. After that, the chemical blowing agent and sulfur are mixed with rubber compound by using two-roll mill. Our experiment is designed by

mixing all chemicals in one step to reduce the procedure of mixing. However, this process should be ensured that sulfur vulcanization does not occur during mixing, thus sulfenamide accelerators with scorch delay mechanism are advantageous. Another reason is that the delayed scorch time plays a key role when rubber compound is compressed in the mold because rubber should have enough time to fill in the mold before crosslinking together. The delayed scorch time takes place by sulfurating species reacted with persulfenyl radical to crosslink precursor. The crosslink precursor rearranges itself to form persulfenyl radical. The persulfenyl radical can either react with another rubber molecule to form crosslink network or reacts with sulfurating species again to form crosslink precursor. In this mechanism, the reduction of persulfenyl radical species reduces free radical to attract other rubber molecules. Therefore, crosslink network is delayed and scorch time is prolonged [18]. This mechanism is shown in Figure 2.2.

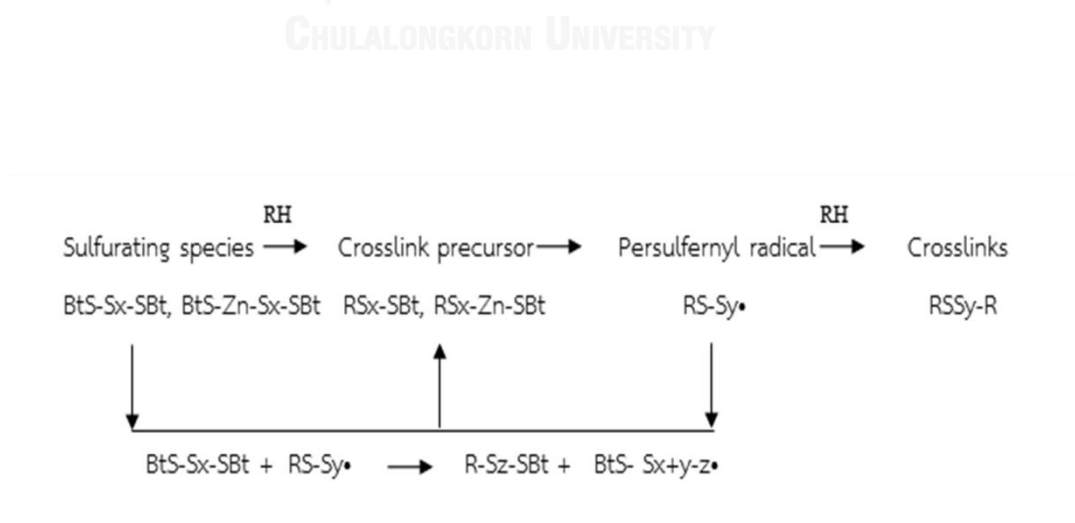


Figure 2.2 Scorch delay mechanism of sulfenamide accelerators [18]

In industries, four sulfenamide accelerators are commonly used including N-cyclohexyl benzothiazole-2-sulfenamide (CBS), N-t-butylbenzothiazole-2-sulfenamide (TBBS), 2-morpholinothiobenzotiazole (MBS) and N-dicyclohexyl benzothiazole-2-sulfenamide (DCBS). In our research, DCBS accelerator which has the slowest respond speed is not selected because natural rubber compound with this accelerator could not be used to fabricate to natural rubber foam (NRF) specimen due to cracking layer of specimen from incomplete crosslink reaction. The effect of chemical structures of alkyl chain and amine functional species in sulfenamide accelerators [18] which is displayed in Figure 2.3 is interested in this research because it might show different sulfur vulcanization rate affecting the properties of NRF specimen.

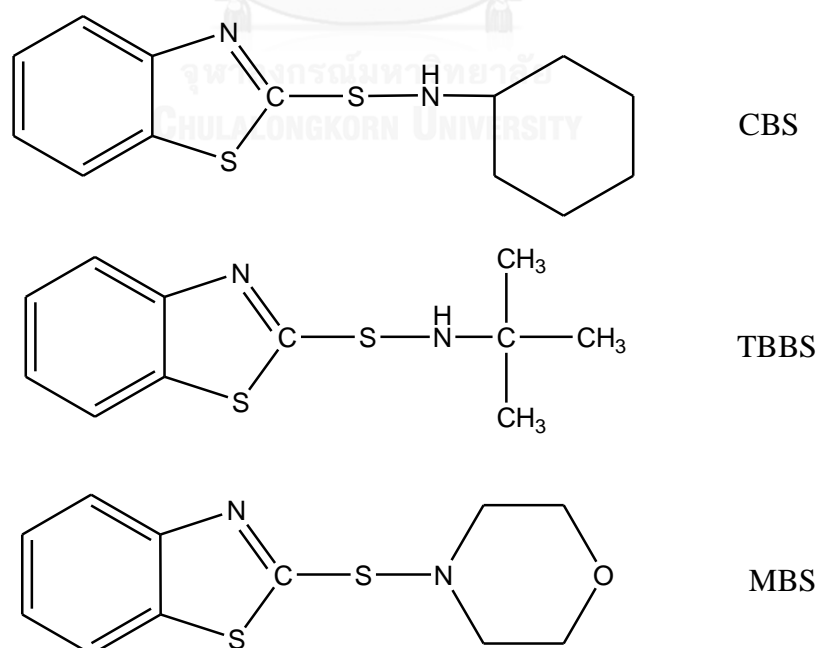


Figure 2.3 The chemical structures of sulfenamide accelerators

In addition to general chemicals in sulfur vulcanization that should be concerned such as type of accelerator [19, 30] and sulfur content [9], there are other factors that relate to sulfur vulcanization rate in natural rubber foam system including processing temperature, types and content of chemical blowing agent and types and content of filler in rubber foam composites [9, 17, 31-33]. The selected processing temperature in this research is limited by the decomposition temperature of chemical blowing agent and degradation temperature of natural rubber. From Arrhenius' equation, high processing temperature results in fast crosslink reaction from high reaction rate constant. In case of chemical blowing agent, different types of chemical blowing agent could produce different types and volume of gas as well as by-products from decomposition reaction. Wimolmala et al. [34] and Najib et al. [35] reported that high amount of some chemical blowing agent could accelerate sulfur vulcanization of rubber foam system. Thus, chemical blowing agent content is varied in this work to understand and to optimize the condition to produce NRF specimen.

### **2.3. Thermal decomposition of chemical blowing agent**

Besides sulfur vulcanization, the thermal decomposition of chemical blowing agent which is the important reaction to produce sponge rubber during compression of natural rubber compound in the mold should be concerned. There are several

types of chemical blowing agent that can be used such as sodium bicarbonate, 4,4-oxydibenzenesulfonyl hydrazide (OBSH), p-toluenesulfonyl semicarbazide, 5-phenyl tetrazole, dinitroso pentamethylene tetramine (DPT) and azodicarbonamide [4, 34-39]. Among these chemical blowing agents, azodicarbonamide is chosen in this work due to its low price with low thermal decomposition temperature. This blowing agent produces nitrogen and carbon monoxide gas to form bubbles in the rubber matrix. In addition, it produces ammonia and amine derivatives [8, 40-42]. Several researchers investigated the effects of content and types of chemical blowing agent on properties of elastomeric materials [34, 35, 39, 43-45]. However, the effect of azodicarbonamide content on cure characteristics and properties of foam product in term of cell density, mechanical and thermal properties have not been investigated from the best of our knowledge.



#### **2.4. Effect of filler on sulfur vulcanization**

Unmodified natural rubber foam exhibits low mechanical and thermal properties for being use in industries. Thus, some fillers have been added such as silica [9, 34], calcium carbonate [32] and carbon black [31, 36, 46-50] to improve elastomer's properties. The level of reinforcing effect of filler in elastomer relates to the geometry of particle because it depends on the volume fraction of particle in rubber matrix, mechanical properties of pristine filler and interaction between filler



particle and rubber matrix [51]. Excellent properties of elastomer nanocomposites can be achieved by the presence of carbon nanoparticle [5, 33, 52-72] because carbon nanoparticle shows higher surface area, thermal and electrical properties than micron-sized carbon particle. Although the diameter of carbon black particle, which is commonly used as carbon filler in industries, is around 20 nanometer, carbon black/elastomer composites shows low mechanical properties because carbon black agglomerates and forms as a cluster or three dimensional aggregate during processing [3, 7, 51]. The incorporation of elastomer with graphene nanoparticle, a two-dimensional carbon nanomaterial, showed higher mechanical properties of elastomer nanocomposites than that with carbon black as reinforcing filler. Ozbas et al. [73] reported that adding only 1 %wt of graphene in natural rubber and styrene-butadiene rubber improved the mechanical properties similar to adding 16 wt% of carbon black in rubber matrix. Zhao et al. [72] also found that natural rubber nanocomposites containing only 0.1 phr of graphene oxide showed tensile strength similar to the composite with 30 phr of carbon black. Although carbon nanotubes has attracted great attention in the development of elastomer nanocomposites, Fu et al. [52] reported that rubber/graphene nanocomposites had higher reinforcing effect than rubber/carbon nanotubes nanocomposites because it has stronger filler-polymer interaction than carbon nanotubes owing to the entanglement between carbon nanotubes resulting in poor dispersion [51]. From this reason, graphene is chosen as filler in our research. However, NR/graphene nanocomposite foam still

shows agglomeration due to high interaction between graphene particles. This is the important problem for optimizing NR/graphene nanocomposite foam's properties. To solve this problem, surface modification of graphene is determined.

Surface modification method of particle can be divided into two main processes that are physical surface modification and chemical functionalization. Physical surface modification is the process of surface treatment by using physical interaction between particle and dispersing agent or surfactant. The physical bonding might be  $\pi$ - $\pi$  interactions, hydrogen bonding or hydrophobic attractions which are relatively weak and unstable [74-76]. Thus, this technique is not appropriate for rubber compounding process with high shear force mixing. Another method is the chemical functionalization of particle with organic molecules. This technique is more efficient than the physical surface modification due to the covalent bonding of organic molecules. The chemical functionalization of graphene with organic molecules includes the free radical addition to the  $sp^2$  carbon atom and covalent modification by using dienophiles [76]. Free radical addition of diamine via diazonium reaction was chosen for treating graphene surface because this process used one-pot reaction with low reaction temperature and short reaction time [77-80]. In this work, graphene was treated with cyclohexyl diamine via diazonium reaction with the same method of Chidawanyika et al. [81] and Ellison et al. [82] who used this reaction to treat carbon nanotube's surface.

Besides the improvement of mechanical and thermal properties of NR/graphene nanocomposite foam by reinforcing effect, adding carbon nanomaterial affects sulfur vulcanization reaction in different ways according to the structure and chemical functional groups on carbon nanomaterial's surface. For example, De falco et al. [83] found that styrene butadiene rubber/carbon nanotubes nanocomposites reduced sulfur vulcanization rate. They suggested that this might be due to the adsorption of accelerator on carbon nanotubes' surface. On the other hand, Sui et al. [63] and Nakaramontri et al. [56] revealed that NR/carbon nanotubes nanocomposites showed faster sulfur vulcanization rate than vulcanized natural rubber without filler. They suggested that it might be caused by the increase of thermal conductivity by pristine carbon nanotubes. Moreover, acid treatment with ball-mill of carbon nanotubes increased sulfur vulcanization rate owing to the small particle size and surface functional groups of treated carbon nanotubes [63]. However, a few works on NR/graphene nanocomposites suggested that graphene could accelerate sulfur vulcanization rate caused by either high thermal conductivity and high specific surface area of pristine graphene [53] or the remaining oxygen functional groups of graphene surface acting as the accelerator to form the accelerator-sulfur complex species [65]. It could be concluded that carbon nanomaterial might either accelerate or retard sulfur vulcanization depending on its structure and surface functional groups. This is one of the factors that should be

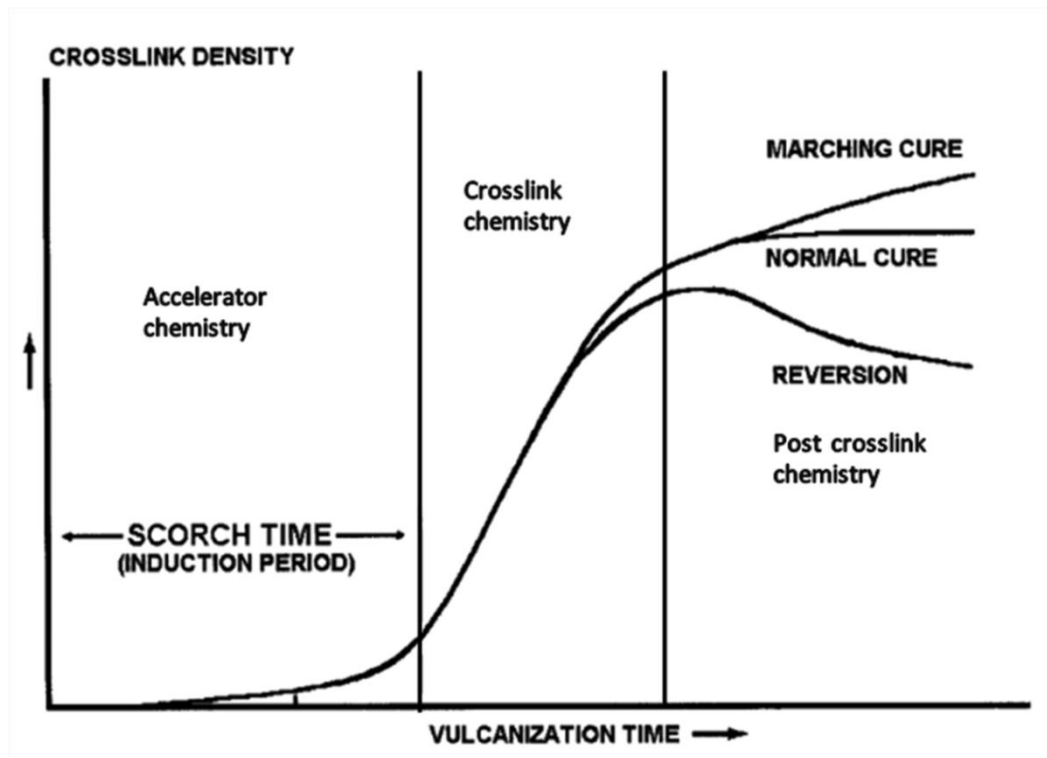
concerned in our work because sulfur vulcanization rate of rubber directly relates to the microvoid structure, crosslink density and the final properties of NRF product.

## 2.5. Cure kinetics and kinetic parameters of natural rubber

After rubber is compounded in an internal mixer, the rheological properties of rubber compound are evaluated to determine cure characteristics. In addition, the compression time to produce natural rubber foam specimen in the mold is determined by the cure time obtained from rheograph. The cure characteristics from rheograph is presented in three steps which are scorch time period, cure time period and post cure time period. Scorch time period is the time in which the accelerator, activator and sulfur form complex chemistry before rubber molecules crosslinking together. Cure time period is the time in which the crosslink chemistry forms three dimensional networks of rubber molecules. During cure time period, crosslink density of rubber rapidly increases which can be observed by measuring the increment of torque. From this period, the degree of cure ( $X$ ) and cure rate ( $\frac{dX}{dt}$ ) can be calculated by comparing the difference between minimum and maximum torque. Kinetic parameters including reaction order ( $m$ ,  $n$ ), cure rate constant ( $K$ ) and activation energy ( $E_a$ ) are also calculated from the data in this period. The final period is the post cure time period which is the post crosslink chemistry. Cure characteristics of this period depends on the accelerator to sulfur molar ratio and

types of filler. It might show marching cure, normal cure and reversion [1, 84, 85].

The cure characteristics from rheograph can be seen in Figure 2.4.



CHULALONGKORN UNIVERSITY  
Figure 2.4 Cure characteristics of rubber [1]

In post cure time period, the mono and di sulfur linkage occur when the concentration of accelerator is higher than that of sulfur. This indicates the normal cure characteristics since mono and di sulfur linkage has a strong bond energy meaning that it could not be easily broken. The heat in process is not high enough to break it, thus crosslink density does not change after it was in that temperature

continuously. On the other hand, the reversion occurs when sulfur concentration is higher than that of accelerator. As a result, the poly sulfur linkage occurs and it is easy to break because bond energy between sulfur molecules is lower than bond energy between carbon-sulfur resulting in the degradation of network [86]. This mechanism results in a reduction of crosslink density after continuous obtaining energy in post cure time period. For marching cure, it is found that some fillers or some chemicals could be linked with three dimensional structure to form the strong network which means high rubber linkage after complete crosslink reaction by sulfur [1, 7, 18, 87] .

In this work, concentration of accelerator is controlled to be higher than sulfur since the strength of vulcanized rubber should not drop when heat is supplied after complete cure [1, 7, 12]. This is the significant characteristics concerned in the production of automotive part due to heat contact of specimen during being used. Moreover, kinetic parameters are investigated only during cure time period as mentioned earlier. The kinetics of scorch time period and post cure time period is neglected. According to the mechanism of sulfenamide accelerators with scorch delay response, the reaction of crosslink rubber molecules indicates the auto catalytic reaction which is the mechanism of the prior product reacts with reactant to form the final product, thus the cure rate at the beginning of cure time period is low because of low level of intermediate species. Cure rate at the intermediate of cure

time increases because it has more persulfanyl radical species. The reduction of cure rate occurs again at almost complete cure of reaction due to less persulfanyl radical species. In general for auto catalytic reaction, the equation that could be used to fit and explain this behavior is revealed as follow [18, 88-91].

$$\frac{dX}{dt} = K(T)X^m(1-X)^n \quad (1)$$

When  $\frac{dX}{dt}$  = Cure kinetic rate of reaction

$K(T)$  = Rate constant

$X$  = Degree of cure

$m, n$  = reaction order

The rate constant depends on reaction temperature which could be explained by Arrhenius's equation in equation (2).

$$K(T) = A \exp \frac{-E_a}{RT} \quad (2)$$

When  $K(T)$  = Rate constant

$A$  = Pre-exponential factor

$E_a$  = Activation energy

$R$  = Universal gas constant (8.314 J/mol.K)

$T$  = Reaction temperature (K)

In addition to the cure kinetics of sulfur vulcanization, other factors such as morphology, mechanical and thermal properties of NRF specimen should be concerned.

## 2.6. Parameters that affect properties of natural rubber foam

There are five main factors of natural rubber foam produced by chemical blowing agent technique affecting rubber foam's properties including blowing agent type, gas volume per mass and concentration of chemical blowing agent, processing temperature, filler and cure kinetics. Firstly, different types of chemical blowing agent show different kinds of gas production which give different gas expansions. Several chemical blowing agents in the market produce different kinds of gas and by-products from the reaction. For example, oxybis (benzene sulfonyl) hydrazide or OBSH degrades to nitrogen gas and produces water vapor as by-product. Sodium bicarbonate degrades to carbon dioxide gas. Azodicarbonamide degrades to nitrogen, carbon monoxide and carbon dioxide gas with amine derivatives as by-products [34-36, 92]. Although the type of chemical blowing agent is similar, many commercial grades would show different characteristics. Secondly, gas volume per mass of chemical blowing agent and the content of blowing agent cause gas concentration in rubber matrix differently. Thirdly, high processing temperature results in large

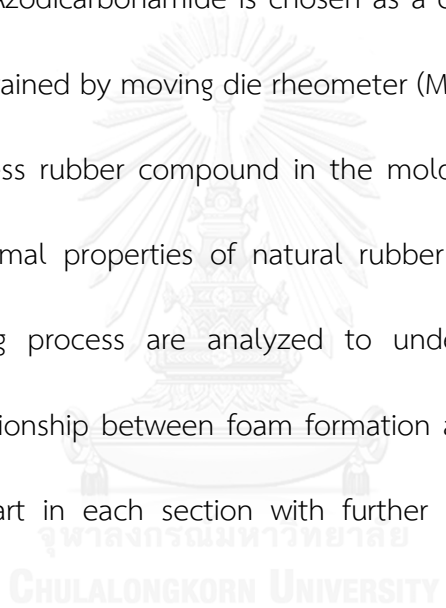


bubble size from high gas expansion. This affects mechanical and thermal properties of natural rubber foam product. In general, the processing temperature is limited by decomposition temperature of chemical blowing agent. However, the chosen type of chemical blowing agent and processing temperature depend on the type of rubber because the processing temperature should not be higher than degradation temperature of rubber which impact the properties of rubber foam product. Another factor is the presence and types of filler which can accelerate or retard sulfur vulcanization and it can be reinforced rubber matrix differently due to different level of filler-rubber interaction. Furthermore, the functional chemistry of filler's surface could affect sulfur vulcanization rate since functional surface of filler could accelerate the crosslink chemistry in sulfur vulcanization [9, 31, 62, 92]. Lastly, the cure kinetics affects the strength of crosslink network and bubble growth mechanism. The suitable cure rate could produce strong crosslink and control bubble size resulting in better rubber foam properties [9, 92-94].

### CHAPTER III

#### EXPERIMENTS

In this research, cure kinetics and kinetic parameters of sulfur vulcanization are studied by varying concentration of chemical blowing agent, types of sulfenamide accelerator and the presence of graphene with and without surface treatment with cyclohexyl diamine. Azodicarbonamide is chosen as a chemical blowing agent. Cure characteristics are obtained by moving die rheometer (MDR) and using cure time from rheograph to compress rubber compound in the mold. The morphology, physical, mechanical and thermal properties of natural rubber foam (NRF) specimen from compression molding process are analyzed to understand the bubble growth mechanism and relationship between foam formation and sulfur vulcanization. The experimental flowchart in each section with further characterization is shown in Figure 3.1.



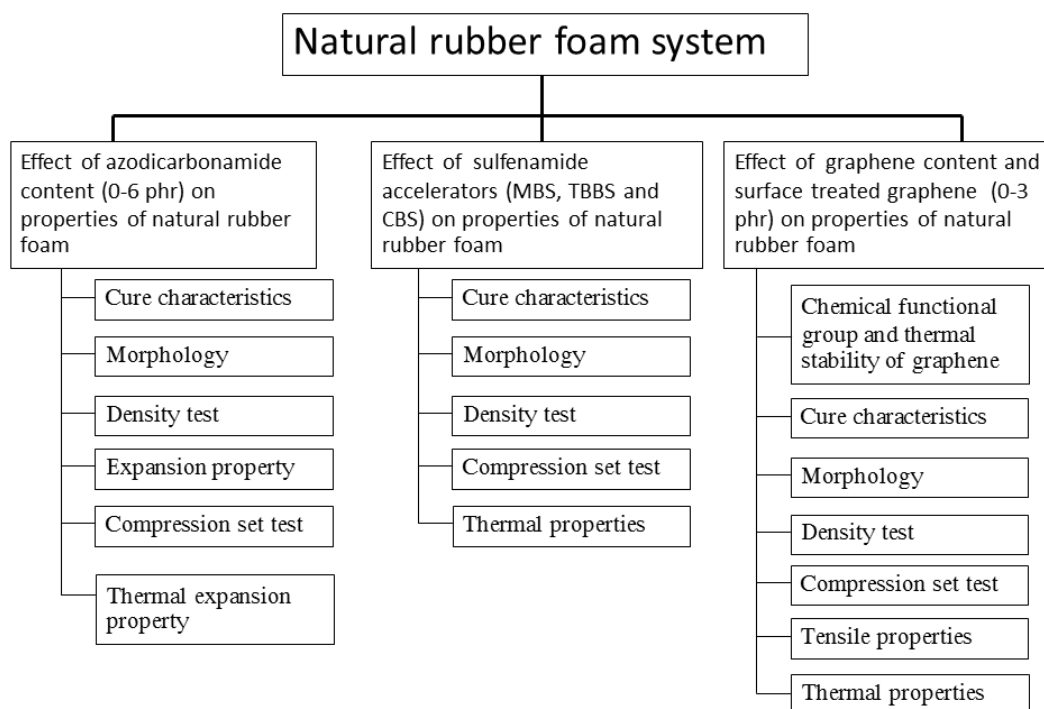


Figure 3.1 The experimental flowchart of natural rubber foam

### 3.1. Materials

In this research, air dried natural rubber sheet with Mooney viscosity (ML1+4 at 100°C) around 66.77 Mooney unit was purchased from Rayong province, Thailand. Sulfenamide accelerators including N-cyclohexyl benzothiazole-2-sulfenamide (CBS), N-t-butylbenzothiazole-2-sulfenamide (TBBS) and 2-morpholinothiobenzotiazole (MBS) were supported by Sunny World Chemical Co., Ltd., Behn Mayer Co., Ltd., Thailand and Akochem Corporation, USA. Other chemicals for sulfur vulcanization system such as ZnO, stearic acid and sulfur were commercial grade.

Azodicarbonamide, chemical blowing agent, with degradation temperature around  $148\pm 3^{\circ}\text{C}$  was supported by AF Goodrich chemical Co., Ltd., Thailand. Graphene nanoplatelet (industrial grade) was purchased from Cheap Tubes Inc., USA. Other chemicals for surface treatment of graphene including trans-1, 4-cyclohexane diamine, sulfuric acid, sodium nitrite ( $\text{NaNO}_2$ ) and N, N-dimethylformamide (DMF) were purchased from ICI Americas Inc., Fisher Scientific, and Sigma-Aldrich, USA.

### 3.2. Sample preparation

#### 3.2.1. Surface treatment of graphene by cyclohexyl diamine via diazonium reaction

Graphene was treated with cyclohexyl diamine via diazonium reaction [81, 82]. Briefly, 90 mg of graphene nanoplatelet was mixed with 120 mg of sodium nitrite ( $\text{NaNO}_2$ ) and 180 mg of trans-1, 4-cyclohexane diamine in 6 ml of sulfuric acid. Then, it was heated at  $80^{\circ}\text{C}$  and stirred at 300 rpm for 1 hour by magnetic stirrer. After cooling the solution down to room temperature, it was filtrated and washed with N, N-dimethylformamide several times by suction filter process with glass fiber membrane (Sterlitech Corporation, USA) until the colorless filtrated solution was obtained. Next, it was washed with DI water to remove any chemical and solvent that might remain from synthesis and washing process and dried in a vacuum oven at  $80^{\circ}\text{C}$  overnight.

### 3.2.2. Natural rubber compounding process

The air dried natural rubber sheet was added in an internal mixer at 80°C and 60 rpm of rotor speed for 2 minutes. Then, it was mixed with other chemicals continuously for 8 minutes. The ratio of accelerator to sulfur was fixed at 5 to 1 by weight to produce the normal cure characteristics after complete crosslink reaction. After mixing, rubber compound was left overnight at room temperature for releasing the stress of rubber molecules during mixing before testing cure characteristics or compressing it in the mold. The chemical compositions in this research are divided into three main parts including the rubber compound with 0-6 phr of azodicarbonamide content in MBS accelerator system, the rubber compound with different sulfenamide accelerators at 4 phr of azodicarbonamide content and the rubber compound with 0-3 phr of graphene and surface treated graphene at 5 phr of azodicarbonamide content in CBS accelerator system as shown in Table 3.1. The natural rubber compound at 4 phr of azodicarbonamide in the second part with CBS accelerator systems (NRF-CBS-B4 and NRF-CBS2-B4) are varied at 2.5 and 2.775 phr of CBS accelerator respectively to study the influence of reactive site from different accelerator to sulfur molar ratio. NRF-CBS2-B4 has similar accelerator to sulfur molar ratio as NRF-TBBS-B4 which is the highest molar ratio among sulfenamide accelerators due to the lowest molecular weight per gram of TBBS accelerator.

Table 3.1 The chemical composition of rubber compound

Sample name	Steric acid (phr <sup>*</sup> )	ZnO (phr)	Sulfur (phr)	accelerator (phr)	CBA <sup>*</sup> (phr)	Graphene	
						UG <sup>*</sup> (phr)	CG <sup>*</sup> (phr)
VNR-MBS	2	5	0.5	2.5	0	0	0
NRF-MBS-B3	2	5	0.5	2.5	3	0	0
NRF-MBS-B4	2	5	0.5	2.5	4	0	0
NRF-MBS-B5	2	5	0.5	2.5	5	0	0
NRF-MBS-B6	2	5	0.5	2.5	6	0	0
NRF-TBBS-B4	2	5	0.5	2.5	4	0	0
NRF-CBS-B4	2	5	0.5	2.5	4	0	0
NRF-CBS2-B4	2	5	0.5	2.775	4	0	0
NRF-CBS-B5	2	5	0.5	2.5	5	0	0
NRF-CBS-B5-UG1	2	5	0.5	2.5	5	1	0
NRF-CBS-B5-UG2	2	5	0.5	2.5	5	2	0
NRF-CBS-B5-UG3	2	5	0.5	2.5	5	3	0
NRF-CBS-B5-CG3	2	5	0.5	2.5	5	0	3

phr = Part per hundred of rubber, CBA = Azodicarbonamide content, UG = Untreated

graphene, CG = Graphene treated with cyclohexyl diamine

### 3.2.3. Compression molding process of natural rubber foam

The rubber compound was compressed into 17x100x5 mm<sup>3</sup> of dimensions. The cure time obtained from rheograph was used for producing natural rubber foam

specimen at 20 bars of pressure in compression molding process. The specimen from this process was used to observe morphology and test mechanical and thermal properties of natural rubber foam specimen.

### 3.3. Characterizations

#### 3.3.1. Mooney viscosity

Air dried natural rubber sheet was cut into circular shape around 5x5 square centimeters and inserted in Mooney viscometer (Alpha's technologies, TechPro ViscTech+, USA) with large rotor size (5 x 5 square centimeters of diameter). The viscometer was tested at 100°C after preheating for 1 minute. After that, it was performed at this condition for 4 minutes to collect the final viscosity of natural rubber. This technique was set following ASTM D1646 standard. The result of this test is shown in Appendix A.

#### 3.3.2. Functional group analysis of graphene nanoplatelet

Graphene and surface treated graphene were characterized to confirm the functional groups on the surface of graphene after treatment. The chemical functional groups of graphene with and without treating with cyclohexyl diamine were identified by using Fourier Transform Infrared (FTIR) spectroscopy in

transmission mode. (Alpha, Alpha-P Bruker optics, USA) The defect on graphene surface from synthesis was evaluated by Raman spectroscopy with 532 nm Nd:YAG laser source (Horiba, LabRam HR Micro Raman Spectrometer, Japan). Moreover, thermal stability of graphene particle was measured by thermogravimetric analyzer (TA instrument, Q50, USA) under nitrogen gas flow with 10°C/minute of heating rate.

### 3.3.3. Cure characteristics

About 4-5 grams of rubber compound was sampled and measured cure characteristics by moving die rheometer (Alpha's technologies, TechPro RheoTechMD+ and MDR 2000, USA) at 1 Hz of frequency, 155-170°C of processing temperature with isothermal condition for 30-50 minutes. The data from rheograph was displayed by on-line computer connected with rheometer. From this data, degree of cure and cure rate were calculated from equations (3) - (6).

$$X(t) = \frac{T_t - T_{\min}}{T_{\max} - T_{\min}} \quad (3)$$

Where  $X(t)$  = Degree of cure

$T_t$  = Torque at time of measurement

$T_{\max}$  = Maximum Torque

$T_{\min}$  = Minimum Torque



Cure rate ( $\frac{dX}{dt}$ ) can be calculated from three point differential numerical

method as follow.

$$\frac{dX}{dt} = \frac{-3X_i + 4X_{i+1} - X_{i+2}}{2\Delta Z} \quad \text{Initial stage} \quad (4)$$

$$\frac{dX}{dt} = \frac{X_{i+1} - X_{i-1}}{2\Delta Z} \quad \text{Medium stage} \quad (5)$$

$$\frac{dX}{dt} = \frac{X_{i+2} + 4X_{i+1} - 3X_i}{2\Delta Z} \quad \text{Final stage} \quad (6)$$

Cure rate ( $\frac{dX}{dt}$ ) from this process was used to calculate kinetic parameters in terms of the cure rate constant (K) and the reaction order (m, n) via curve fitting method by MathLab program. The activation energy ( $E_a$ ) was obtained by using Arrhenius' equation related to the cure rate constant (K) with different processing temperatures and it was explained how easily the crosslink reaction by sulfur could be occurred.

#### 3.3.4. Solvent absorption and gel content during sulfur vulcanization reaction

The crosslink reaction of rubber molecules during sulfur vulcanization of vulcanized natural rubber with MBS accelerator (VNR-MBS) was analyzed by submerging the vulcanized natural rubber in toluene for one week. VNR-MBS specimens were tested by moving die rheometer (MDR) with various vulcanization

times at 15, 20, 25 and 30 minutes which were time of curing period of this formula and submerged them into 200 ml of toluene for one week. After that, the specimen was filtrated by suction filtration process and weighed it before and after drying in a vacuum oven at 80°C overnight to find the solid content and mass percentage of swelling based on dried rubber content after swelling. The result of this section can be seen in Appendix B.

#### 3.3.5. Morphology

The rubber foam specimen from compression molding process was dipped into liquid nitrogen and fractured. Then, it was bound onto the substrate by using carbon paint and left at least 3 hours at room temperature for bonding the specimen on the substrate. After that it was coated with gold or platinum particle on surface to obtain conductive surface by sputtering machine for 4 minutes. The conductive sample was inserted into vacuum chamber of scanning electron microscope (SEM) and the images were taken by using accelerating voltage around 10-15 kV. (JEOL, JSM-5400 and JSM-7401F, Japan). The bubble diameter and size distribution of bubbles were calculated from SEM images by assuming spherical bubble in rubber matrix and using ferret diameter for analysis.

The degree of dispersion of graphene particle in vulcanized natural rubber at 3 phr of graphene with and without surface treatment was observed by transmission electron microscopy (TEM) at 200 kV of accelerating voltage (FEI, Technai G2 20S-Twin, USA). The rubber compound was compressed in square mold. The sample was cut under cryogenic condition by ultrathin microtome (RMC, MTX75500, USA) with 70-90 nm of specimen's thickness and using copper grid as a conductive substrate.

### 3.3.6. Cell density calculation

Bulk density and skeleton density of natural rubber foam (NRF) were determined by using densitometer (Mirage, MD 200S, Japan) and gas pycnometer (Micromeritics, AccuPyc II 1340 and 1330, USA) respectively. The cell density of NRF product was calculated from equation (7) and (8) respectively.

$$Porosity = 1 - \frac{\rho_b}{\rho_s} \quad (7)$$

$$\rho_{cell} = \frac{Porosity}{Volume_{gas}} \quad (8)$$

Where  $\rho_b$  = Bulk density

$\rho_s$  = Skeletal density

$\rho_{cell}$  = Cell density

### 3.3.7. Tensile properties and compression set

NR/graphene nanocomposite foam was compressed in square mold and cut as dumbbell shape. The specimen was prepared following ASTM D412 Die C standard and the tensile properties were collected at 500 mm/min of crosshead speed with 1 kN of loading (Instron, Instron5567, USA). Furthermore, the compression set test of natural rubber foam specimen was measured following ASTM D395 Method B (70°C, 22 h) standard to observe the resistance of rubber foam during applying compressive stress.

### 3.3.8. Thermal properties

The thermal expansion coefficient of vulcanized natural rubber and natural rubber foam specimen were measured by thermo mechanical analyzer. (Perkin Elmer, Pyris diamond TMA, USA). The specimen from compression molding process was cut into 0.5x0.5 square centimeters and inserted it in the chamber. Then, the testing temperature was increased from 30°C to 120°C at 5°C/min of heating rate. The force that pressed on the specimen was set at 5 mN during the test.

The thermal conductivity of natural rubber foam specimen was evaluated by using thermal constant analyzer with a kapton insulation disk (Hot Disk, Hot Disk AB, Sweden and Laser Comp Inc, Fox 200, USA). The specimen was cut into a square

shape with 5-10 millimeters of thickness. The specimen was run at room temperature condition.



Table 3.2 Measurement and characterization of sample

Instrument	Specification	Characterizations
Mooney viscometer	Alpha's technologies, TechPro ViscTech+, USA	Viscosity
Fourier Transform Infrared (FTIR) spectroscopy	Alpha, Alpha-P Bruker optics, USA	Functional group on surface of graphene
Raman Spectroscopy	Horiba, LabRam HR Micro Raman Spectrometer, Japan	Defects on surface of graphene
Themogravimetric analyzer	TA instrument, Q50, USA	Thermal decomposition Temperature
Moving Die Rheometer (MDR)	Alpha's technologies, TechPro RheoTechMD+ and MDR 2000, USA	Cure characteristics
Scanning Electron Microscopy (SEM)	JEOL, JSM-5400 and JSM-7401F, Japan	Morphology
Transmission Electron Microscopy (TEM)	FEI, Technai G2 20S-Twin, USA	Graphene dispersion
Densitometer	Mirage, MD 200S, Japan	Bulk density
Pycnometer	Micromeritics, AccuPyc II 1340, USA	Skeleton desity
Instron	Instron, Instron5567, USA	Tensile properties
Thermo mechanical analyzer (TMA)	Perkin elmer, Pyris diamond TMA, USA	Thermal expansion coefficient
Thermal constant analyzer	Hot Disk, Hot Disk AB, Sweden and Laser Comp Inc, Fox 200, USA	Thermal conductivity

## CHAPTER IV

### RESULTS AND DISCUSSION

There are many factors for controlling size of natural rubber foam specimen as mentioned in the literature. The development of natural rubber foam (NRF) in this research only focused on the gas volume from decomposition of chemical blowing agent which relates to azodicarbonamide content, the different chemical structures of sulfenamide accelerators, and the effect of filler and surface functional groups of filler on properties of NRF product. Graphene and surface treated graphene with cyclohexyl diamine are used as filler in this research. However, these three factors affect the sulfur vulcanization rate. Thus, our research mainly discusses the influence of kinetics and kinetic parameters from sulfur vulcanization on morphology, mechanical and thermal properties of rubber foam product.

#### **4.1. Effect of azodicarbonamide content on cure characteristics and properties of natural rubber foam**

##### **4.1.1. Effect of azodicarbonamide content on cure kinetics and kinetic parameters of NRF product**

The torque increment of rubber compound with various azodicarbonamide contents from 0-6 phr using MBS accelerator system was measured by moving die

rheometer (MDR). MBS accelerator is used in all rubber compounds of this section because it exhibits the lowest acceleration rate among other sulfenamide accelerators from our preliminary test. Thus, it might show the effect of gas increment obviously at high content of chemical blowing agent. The natural rubber with 6 phr of azodicarbonamide without sulfur vulcanizing agent (NR-B6) was tested to confirm that the increment of torque from rheograph occurred by crosslink network of sulfur in vulcanization reaction as seen in Figure 4.1. From this Figure, the torque of NR-B6 slightly reduces due to the loss of solid content from decomposition of azodicarbonamide and gas bubble effect. This result can confirm that the increase of torque from this measurement causes by the crosslink network by sulfur without the effect from bubble obstruction. Moreover, the level of crosslink network of sulfur with vulcanization over time was also confirmed by submerging specimen in solvent method as discussed in experimental section and the raw data is in Appendix B. It reveals that the solvent absorption decreases while the gel content increases with increasing cure time due to the increases of crosslink network of rubber molecules by sulfur. In Figure 4.1, rheograph of vulcanized natural rubber without chemical blowing shows the longest scorch time and the maximum torque after complete cure. The scorch time ( $t_{s1}$ ) is the delay time of sulfur vulcanization before the rubber molecules are linked and formed three dimensional networks. In this work, the scorch time is defined by one unit of torque increment during measurement. The scorch time of all samples in this section is summarized in Table 4.1. The shorter



scorch time and reduction of torque after complete cure is observed when increasing the content of chemical blowing agent. Moreover, the torque after complete crosslink reaction shows the normal cure characteristics due to high accelerator to sulfur molar ratio. This results in mono or di-sulfur linkage of rubber molecules during sulfur vulcanization. The mono and di-sulfur linkage has higher bond energy than polysulfur linkage because bond energy of C-S bond is higher than that of S-S bond [86]. Thus our system at 155°C of processing temperature shows normal cure after continuously contacting with heat which is useful for using in automotive application or advanced engineering material with heat contact during usage. When increasing the content of chemical blowing agent, the maximum torque of natural rubber foam (NRF) decreases due to high volume of gas bubble in rubber matrix which might reduce the shear force [35, 43]. The maximum torque can be implied the crosslink density because similar minimum torque of rubber compound from rheograph of all formulas is presented. Moreover, NRF-MBS-B5 and MRF-MBS-B6 show slightly different maximum torque due to unchanging microvoid structure of NRF as can be seen in SEM image in section 4.1.2.

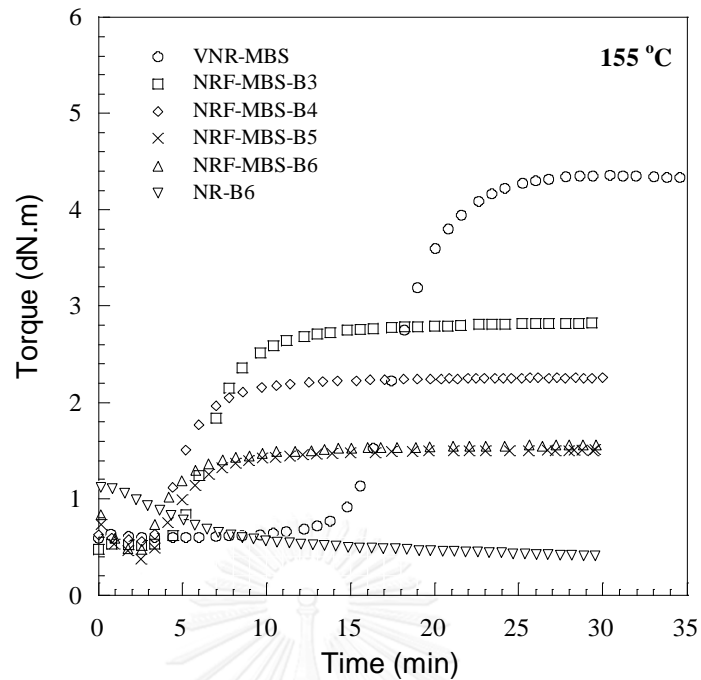


Figure 4.1 Torque measurements of vulcanized natural rubber and natural rubber foam when using MBS accelerator system while varying chemical blowing agent contents at 155°C

During the cure time period, the torque increases with the reaction time owing to crosslinking of rubber molecules by sulfur. The cure time period from torque measurement of rheograph in Figure 4.1 shows S shape indicating low crosslink network at the beginning, rapidly increased crosslink network at the intermediate period and constant torque again (no crosslink reaction anymore) at last. These characteristics are the general autocatalytic reaction. For sulfur vulcanization with sulfenamide accelerator system, the sulfenamide accelerator could be degraded to amine species and formed the sulfurating species with ZnO and steric acid. The

possible mechanism of this process with CBS accelerator was revealed by Wu et al. [65] as can be seen in Figure 4.2.

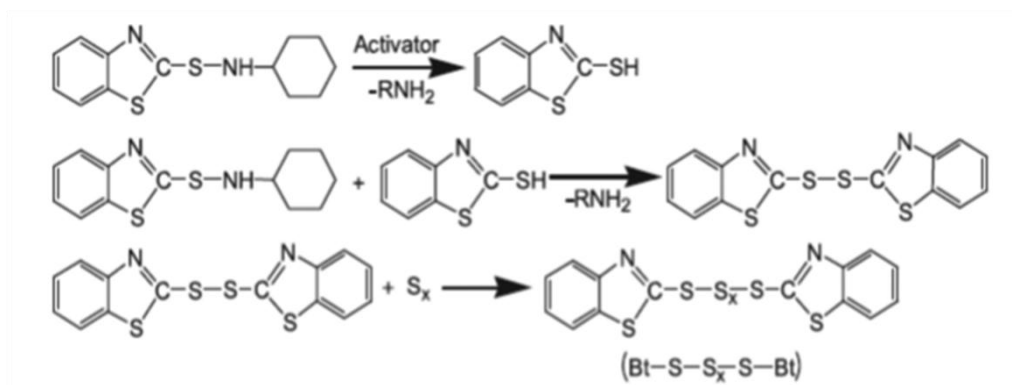


Figure 4.2 Mechanism of sulfuration species of activator with CBS accelerator [65]

The sulfuration species reacts with rubber molecules to form crosslink precursor and it changes the form to persulfenyl radical. The persulfenyl radical can either react with another rubber molecule to form crosslink network or react with sulfuration species again to form crosslink precursor. At the beginning of the last step of this mechanism, slow sulfur vulcanization rate is observed due to high content of sulfuration species. At almost the end of the reaction (almost complete crosslink reaction), slow sulfur vulcanization rate is observed again due to low content of persulfenyl radicals. Furthermore, the cure time period of rubber compound is used to calculate the degree of cure and cure rate of crosslink by sulfur. It is calculated by

using equation (3) - (6) in experimental section. The graph between cure rate and degree of cure of rubber compound with different azodicarbonamide contents is shown in Figure 4.3.

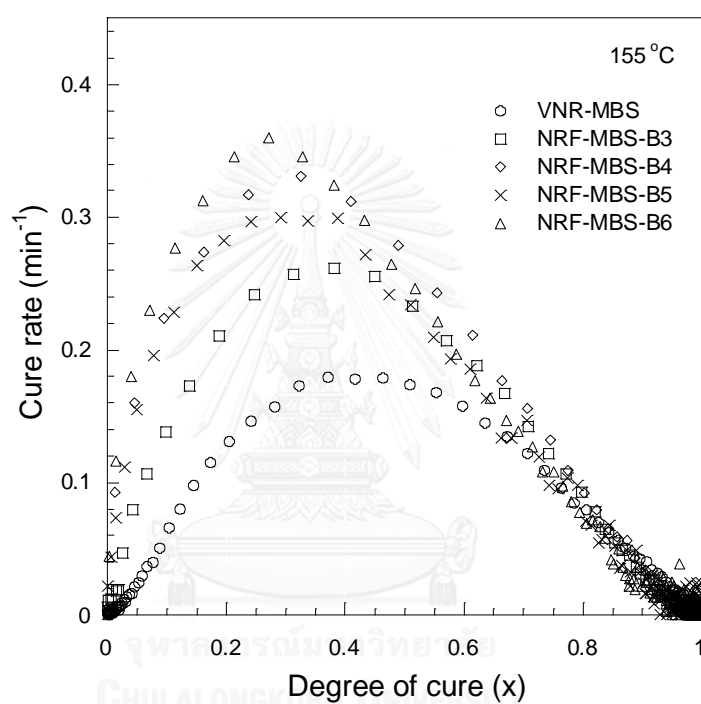


Figure 4.3 Cure characteristics of vulcanized natural rubber and natural rubber foam when using MBS accelerator while varying chemical blowing agent contents at 155°C

From Figure 4.3, the cure rate of sulfur vulcanization increases with increasing the content of chemical blowing agent. The increasing of cure rate might be due to the acceleration of amine derivatives from thermal decomposing of

azodicarbonamide [40-42]. The possible mechanism of azodicarbonamide decomposition is proposed in Figure 4.4. The presence of azodicarbonamide in rubber compound accelerates sulfur vulcanization might be due to the presence of by-products from azodicarbonamide decomposition which are amine derivative which could form complex species similar to sulfenamide accelerator.

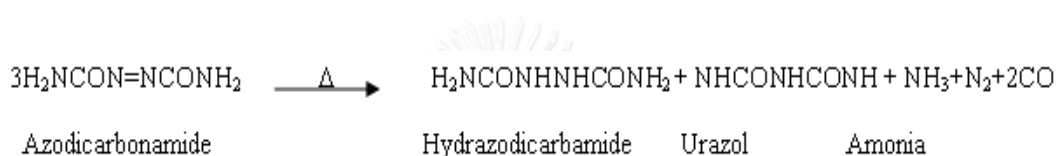


Figure 4.4 The possible mechanism of thermal decomposition of azodicarbonamide

[40-42]

The torque of rubber compound was measured with various processing temperature from 155 to 170°C to observe the effect of temperature on cure kinetics and calculate the activation energy ( $E_a$ ) of sulfur vulcanization with different azodicarbonamide contents. Figure 4.5 and 4.6 are the example of torque measurement and cure characteristics of rubber compound at 3 phr of chemical blowing agent with different processing temperatures. It has been found that the increase of processing temperature reduces scorch time and increases sulfur vulcanization rate. This is because the increase of processing temperature results in

the increase of cure rate constant ( $K$ ) from Arrhenius' law. When the processing temperature further increases, the post cure time period slightly changes to reversion as can be seen in Figure 4.5 due to high energy enough for breaking crosslink network. The other compositions of natural rubber compound are also measured at different processing temperatures and they also show the same trend. The cure rate and degree of cure of each compositions are fitted by Matlab program to obtain the cure rate constant ( $K$ ) and reaction order ( $m$ ,  $n$ ) of sulfur vulcanization.

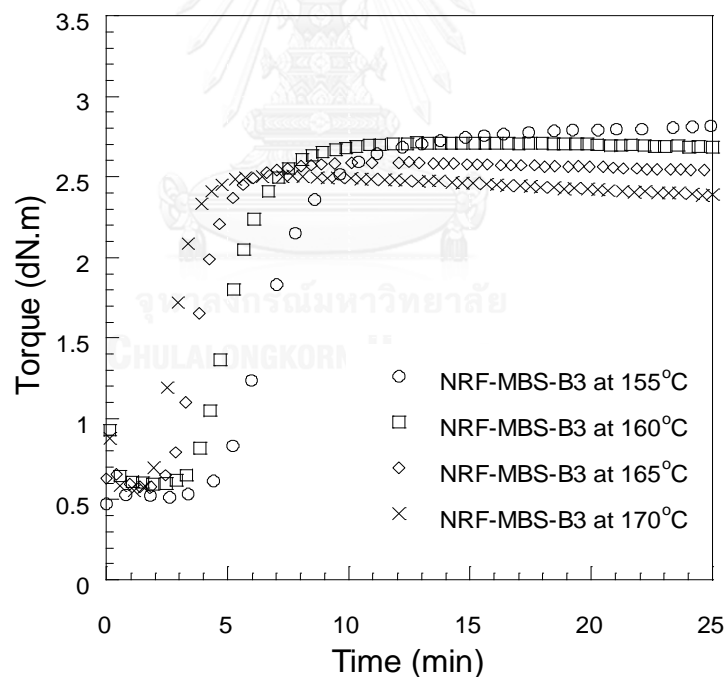


Figure 4.5 Torque measurement of natural rubber foam when using MBS accelerator at 3 phr of chemical blowing agent with various processing temperatures

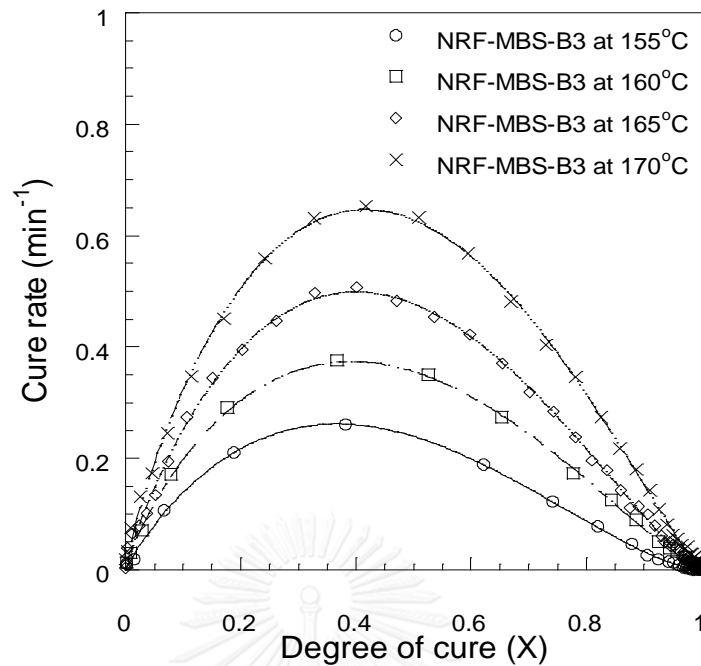


Figure 4.6 Cure characteristics of natural rubber foam when using MBS accelerator at 3 phr of chemical blowing agent with various processing temperatures

After achieving cure rate constant (K) from Mathlab program, activation energy ( $E_a$ ) of sulfur vulcanization in each formulas is calculated from a slope of the graph as illustrated in Figure 4.7. This linear method is applied from Arrhenius 'equation which is shown in equation (2). The summary of cure kinetics and kinetic parameters is shown in Table 4.1.

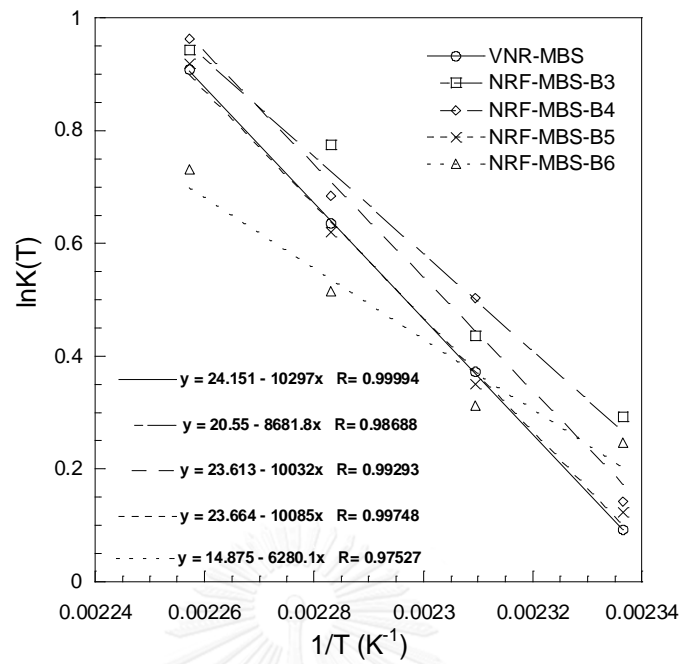


Figure 4.7 The linear plot of  $\ln K(T)$  vs  $1/T$  of vulcanized natural rubber and natural rubber foam when using MBS accelerator with different chemical blowing agent

contents



Table 4.1 Summary of the cure kinetics and kinetic parameters of vulcanized natural rubber and natural rubber foam when using MBS accelerator while varying chemical blowing agent contents

Sample name	$t_{s1}^*$ (min)	$t_{10}^*$ (min)	$t_{c90}^*$ (min)	n order	m order	K(T) (min <sup>-1</sup> )	$E_a$ (kJ/mol)
VNR at 155°C	17.01	15.60	25.70	1.43	1.18	1.09	85.61
VNR at 160°C	12.75	11.60	16.56	1.38	1.19	1.45	
VNR at 165°C	9.01	8.20	11.87	1.36	1.18	1.89	
VNR at 170°C	6.44	5.79	8.68	1.38	1.21	2.48	
NRF-MBS-B3 at 155°C	6.43	4.94	10.48	1.57	0.91	1.34	72.18
NRF-MBS-B3 at 160°C	4.99	3.86	7.12	1.29	0.83	1.55	
NRF-MBS-B3 at 170°C	3.73	2.84	5.29	1.31	0.87	2.17	
NRF-MBS-B3 at 175°C	2.81	2.10	3.86	1.19	0.84	2.57	
NRF-MBS-B4 at 155°C	5.39	3.90	8.48	1.46	0.62	1.15	83.41
NRF-MBS-B4 at 160°C	4.25	3.00	6.73	1.57	0.65	1.65	
NRF-MBS-B4 at 165°C	3.19	2.23	4.84	1.44	0.58	1.98	
NRF-MBS-B4 at 170°C	2.39	1.60	3.59	1.42	0.63	2.62	
NRF-MBS-B5 at 155°C	8.52	3.35	8.96	1.60	0.63	1.13	83.85
NRF-MBS-B5 at 160°C	4.50	2.65	6.31	1.45	0.56	1.42	
NRF-MBS-B5 at 165°C	3.24	2.00	4.48	1.38	0.55	1.86	
NRF-MBS-B5 at 170°C	2.80	1.54	3.45	1.40	0.52	2.50	
NRF-MBS-B6 at 155°C	8.68	2.90	8.74	1.71	0.59	1.28	52.21
NRF-MBS-B6 at 160°C	N/A	2.23	6.24	1.53	0.47	1.37	
NRF-MBS-B6 at 165°C	N/A	1.67	4.33	1.41	0.44	1.68	
NRF-MBS-B6 at 170°C	N/A	1.26	3.48	1.40	0.43	2.08	

\* $t_{s1}$  = scorch time,  $t_{10}$  = time at 10% of torque increment,  $t_{c90}$  = cure time

The scorch time ( $t_{s1}$ ), the time at 10% of vulcanization ( $t_{10}$ ) and cure time at 90% of vulcanization ( $t_{c90}$ ) reduce with increasing processing temperature due to high cure rate constant ( $K$ ) resulting in fast sulfur vulcanization. The scorch time of NRF-MBS-B5 and NRF-MBS-B6 are longer than other compositions of natural rubber foam product because they contain low degree of crosslink network as can be seen in Figure 4.1. The low degree of crosslink of rubber foam specimen at high content of chemical blowing agent results in slight difference between maximum and minimum torque. However, the time at 10 % of vulcanization reduces with the presence of azodicarbonamide referring to the acceleration function of amine derivative from azodicarbonamide decomposition. The  $n$  and  $m$  order of sulfur vulcanization are obtained by fitting experimental data with autocatalytic reaction (Equation (1)) using Matlab program. The term  $X^m$  refers to the rate of reactant disappearance and formation of product. The term  $(1-X)^n$  refers to the formation of hindrance product or intermediate retarding product representing the scorch delay mechanism of sulfenamide accelerator [95, 96]. Thus,  $m$  order might relate to crosslink network of sulfur vulcanization. In Table 4.1, the  $m$  order of NRF reduces when increasing chemical blowing agent content due to low crosslink network by sulfur. The  $m$  order can be used to explain the result of maximum torque of rubber foam product from Figure 4.1 in which the presence of chemical blowing agent reduces crosslink density. Furthermore, the change of  $n$  order at 155°C of processing temperature in each formulas compared to high processing temperatures might be because temperature

is low enough to observe the influence of amine species accelerate the reaction between persulfanyl radical and sulfurating species to form crosslink precursor. On the contrary, the rubber compound at high processing temperature provides high content of amine derivative from azodicarbonamide decomposition. From this reason, the rapid reaction between the persulfanyl radical and sulfating species at high temperature results in unchanging of  $n$  order of autocatalytic reaction. The activation energy ( $E_a$ ) of NRF-MBS-B3 is lower than that of vulcanized natural rubber because of amine fragment from decomposition of chemical blowing agent but when increasing the amount of chemical blowing agent to 4 and 5 phr, the  $E_a$  slightly increases due to the obstruction of high quantity of bubble in rubber matrix which can be seen from the morphology in section 4.1.2. The  $E_a$  of NRF-MBS-B3 is lower than that of NRF-MBS-B4 and NRF-MBS-B5 could be caused by the thicker microvoid structure in the NRF-MBS-B3 specimen which facilitates sulfur vulcanization confirmed by SEM image in section 4.1.2. However, the  $E_a$  of NRF-MBS-B6 is significantly low which might be caused by the low  $R^2$  from linear plot method of Arrhenius's equation representing high deviation of experimental data.

#### 4.1.2. Effect of azodicarbonamide content on morphology of NRF product

Natural rubber compound was compressed in the mold at 155°C which is the suitable condition for preparing natural rubber foam specimen because it is not too high that can degrade rubber molecules but it is high enough to decompose azodicarbonamide. The compression time of the specimen depends on the 90% cure time ( $t_{c90}$ ) of rubber compound obtained from moving die rheograph. The cross sectional fractured surface of the specimen at 3-6 phr of chemical blowing agent is observed by scanning electron microscopy (SEM) to explain how cure characteristics affects the morphology of rubber foam product. In Figure 4.8, the bubble size of NRF-MBS-B3 is larger than that of NRF-MBS-B4 and it also shows thick microvoid structure. The micrograph of NRF-MBS-B3 shows larger bubble size than that of NRF-MBS-B4 which could be due to slow sulfur vulcanization supported by the cure kinetics as discussed in section 4.1.1, resulting in longer time of gas expansion in rubber matrix. The thicker microvoid structure of NRF-MBS-B3 is caused by low gas volume from low chemical blowing agent content. While the content of blowing agent increases from 3 to 4 phr, the bubble size of NRF-MBS-B4 decreases due to fast sulfur vulcanization rate from the effect of amine derivative from chemical blowing agent decomposition. After increasing chemical blowing agent content to 5-6 phr (NRF-MBS-B5 and NRF-MBS-B6), some coalescence of bubbles (inserted circle in

Figure 4.8) are observed due to high gas volume from decomposing of azodicarbonamide. The coalescence between bubbles to form large bubbles in rubber matrix and high gas volume result in low crosslink network of rubber molecules by sulfur indicated by low m order of natural rubber foam at 5-6 phr of chemical blowing agent from kinetic parameters in Table 4.1. It might be concluded from SEM micrograph that the formulation of NRF-MBS-B4 is the optimal condition because the NRF product shows small bubble size with no-coalescence between bubbles. However, only the microvoid structure is not enough to confirm the suitable content of azodicarbonamide in our rubber foam system. Thus, bulk density, volume expansion of specimen after compression in the mold and thermal expansion coefficient should be measured to support before studying the effect of chemical structures of sulfenamide accelerators in section 4.2.

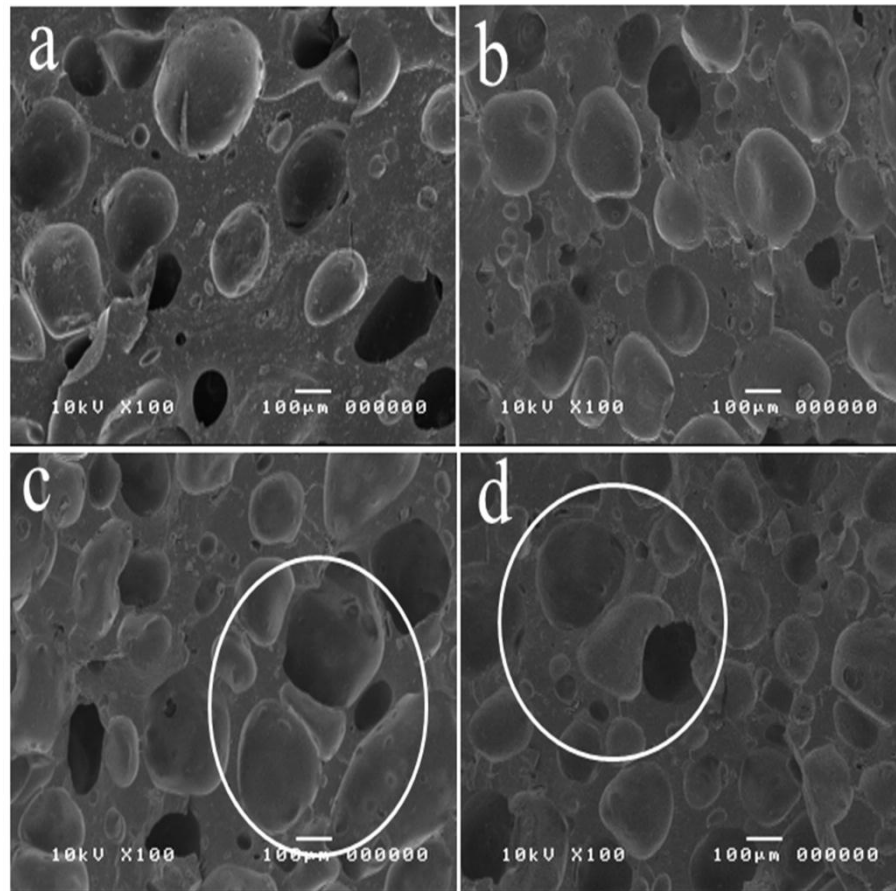
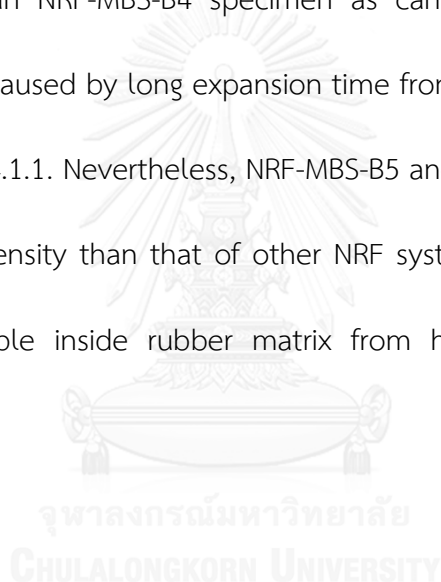


Figure 4.8 SEM images of natural rubber foam specimen produced at 155°C of processing temperature (a) NRF-MBS-B3, (b) NRF-MBS-B4, (c) NRF-MBS-B5, (d) NRF-MBS-B6

#### 4.1.3. Effect of azodicarbonamide on physical and thermal properties of NRF product

The bulk density of natural rubber foam (NRF) produced at 155°C of processing temperature was measured to determine how much of gas could be preserved in

natural rubber matrix. In Figure 4.9, the bulk density of vulcanized natural rubber using MBS accelerator is around  $0.9 \text{ g/cm}^3$  which is the common density of rubber. The bulk density of natural rubber foam significantly drops owing to the gas bubble inside rubber matrix from chemical blowing agent decomposition. NRF-MBS-B3 and NRF-MBS-B4 specimens have the same bulk density. Although NRF-MBS-B4 specimen has higher chemical blowing agent content, NRF-MBS-B3 specimen contains larger bubble diameter than NRF-MBS-B4 specimen as can be seen in SEM images in section 4.1.2. This is caused by long expansion time from slow sulfur vulcanization as discussed in section 4.1.1. Nevertheless, NRF-MBS-B5 and NRF-MBS-B6 specimen have slightly lower bulk density than that of other NRF systems because they have high amount of gas bubble inside rubber matrix from high chemical blowing agent content.



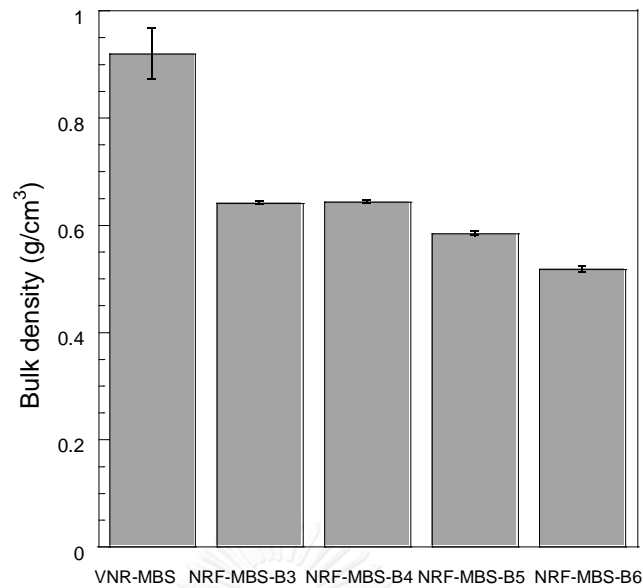


Figure 4.9 Bulk densities of vulcanized natural rubber and natural rubber foam with different chemical blowing agent contents produced at 155°C of processing temperature

The expansion of specimen after removing it from the mold was measured in terms of dimension increment and calculated to the increased volume after leaving specimen overnight for releasing the stress of rubber molecules during compression molding process. The volume of NRF specimen is compared with that of vulcanized natural rubber in term of percentage of volume increment. All specimens were compressed at 155°C. The percentage of volume expansion as shown in Figure 4.10 directly relates to the bulk density because if the bulk density is low, it means high gas volume inside rubber matrix, resulting in high volume expansion of specimen.



From this result, it can be implied that if the controlled size of the specimen is concerned, the bulk density of specimen should be high but it should be considered with morphology of specimen concurrently because high rubber foam density might have large bubble size. The volume expansion of NRF specimen is only measured in this section. The other sections use cell density and morphology to consider the appropriate condition and explain properties of NRF product.

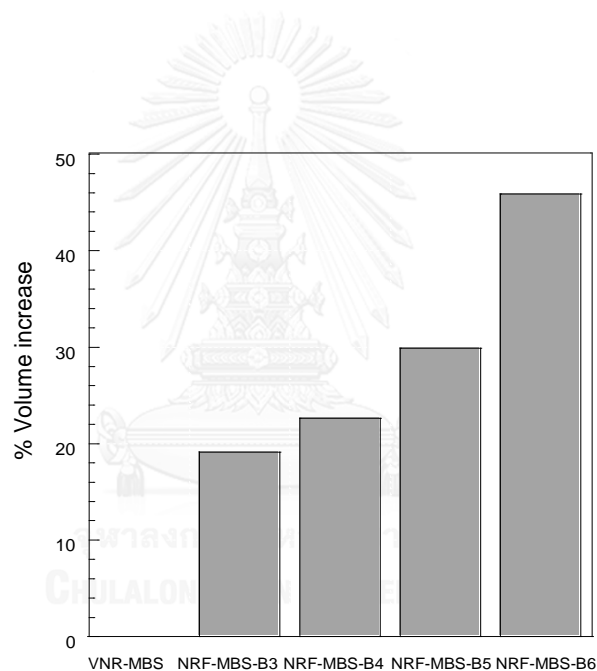


Figure 4.10 Volume expansion of natural rubber foam produced at 155°C of processing temperature compared to that of vulcanized natural rubber

In addition, the thermal expansion coefficient (CTE) of NRF specimen is also investigated. Figure 4.11 shows the CTE of vulcanized natural rubber and natural

rubber foam produced at 155°C of processing temperature with various testing temperature between 40 and 90°C. This temperature range is chosen because it shows linear behavior as a function of temperature. Because of the normal cure characteristics in post cure time period, the thermal property of the specimen does not change during the test. The vulcanized natural rubber has low CTE because it has high crosslink network without gas bubbles inside rubber matrix. After adding chemical blowing agent, the CTE of rubber foam product increases which means it can expand easily after contacting heat due to low crosslink network. The large variation of natural rubber foam with 3 and 6 phr of blowing agent might be caused by the non-uniform of bubbles in rubber matrix. The CTE of NRF-MBS-B4 specimen is the lowest compared to others formulas because it has the smallest bubble size with no coalescence between bubbles. This result also supports that NRF with 4 phr of chemical blowing agent is the optimal condition in this section.

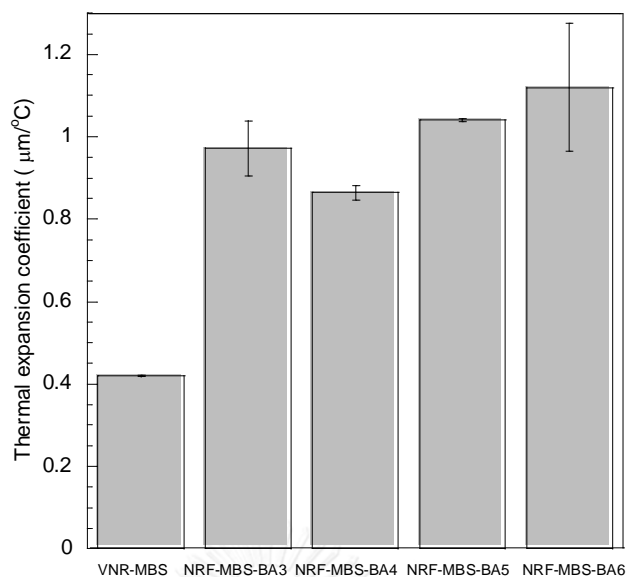


Figure 4.11 Thermal expansion property of vulcanized natural rubber and natural rubber foam produced at 155°C of processing temperature with different chemical blowing agent contents

## 4.2. Effect of sulfenamide accelerators on cure characteristics and properties of natural rubber foam

### 4.2.1. Effect of sulfenamide accelerators on cure kinetics and kinetic parameters of NRF product

Natural rubber compound used in this section was compounded with different sulfenamide accelerators to study the effect of chemical structures of accelerator on sulfur vulcanization rate and properties of natural rubber foam (NRF). The chemical blowing agent was set at 4 phr as mentioned in section 4.1. Chemical

structures of sulfenamide accelerators, i.e., 2-morpholinothiobenzotiazole (MBS), N-t-butylbenzothiazole-2-sulfenamide (TBBS) and N-cyclohexyl benzothiazole-2-sulfenamide (CBS) can be seen in Figure 2.3. Although N-dicyclohexyl benzothiazole-2-sulfenamide (DCBS) is one of the chosen sulfenamide accelerator, the result does not shown in this work because the natural rubber foam containing DCBS accelerator cannot be fabricated due to cracking of specimen after removing it from the mold. This might be due to incomplete crosslink reaction by sulfur from the slowest sulfur vulcanization. From Figure 2.3, MBS accelerator has tertiary amine structure before breaking and forming with ZnO, steric acid and sulfur as sulfurating species while TBBS and CBS accelerator have secondary amine structure with alkyl chain and cyclohexyl ring structure, respectively. From the best of our knowledge, there are no evidences of research about the effect of their structures on properties of rubber foam system. Moreover, sulfur vulcanization rate is the important factor to control bubble size from gas expansion during chemical blowing agent decomposition. Natural rubber compound with CBS accelerator is mixed into two formulas which are NRF-CBS-B4 and NRF-CBS2-B4 in which NRF-CBS-B4 contains 2.5 phr of CBS accelerator while NRF-CBS2-B4 contains 2.775 phr of CBS accelerator. These are used for comparison with the same weight of other sulfenamide accelerators and the same accelerator to sulfur molar ratio with NRF-TBBS-B4 which is the highest one due to low molecular weight of TBBS accelerator respectively. The accelerator to sulfur molar ratio of rubber compound can be seen in Table 4.2. The accelerator to sulfur

molar ratio is concerned because the amount of reactive sites of accelerator might affect sulfur vulcanization rates. Thus, this effect should be controlled. Torque measurement of NRF from moving die rheograph is displayed in Figure 4.12. Rubber compound was tested at 155°C. Its cure rate was calculated by the same procedure as mentioned in section 4.1.1. The plot between cure rate ( $\frac{dX}{dt}$ ) and degree of cure (X) is shown in Figure 4.13. NRF-MBS-B4 shows the longest scorch time with the slowest sulfur vulcanization rate because MBS accelerator has tertiary amine in which nitrogen is a part of cyclic ring while TBBS and CBS accelerator have the secondary amine in their structure. The structure of amine functional group in sulfenamide accelerator is the key role for the speed of sulfur vulcanization because sulfur vulcanization depends on the bond strength of the sulfur-nitrogen bond, stereochemistry and basicity of the amine group after molecules of accelerator are broken down [97]. The amine group from sulfenamide accelerator forms complex species with Zn ion and other chemicals during forming as sulfurating complex. This means that if amine group from sulfenamide accelerator has high basicity, fast sulfur vulcanization could be observed. Nevertheless, the basicity of amine relates to the stability of unpaired electron of nitrogen atom in amine group [98, 99]. Thus, NRF-MBS-B4 exhibits slower sulfur vulcanization rate than other sulfenamide accelerators due to less basicity of tertiary amine in MBS accelerator. For TBBS and CBS accelerator's structure, Rodger et al.[97] reported that the amine fragment of CBS

accelerator structure has the lowest  $pK_b$ , meaning that it has highest basicity. This is the reason why NRF-CBS-B4 shows shorter scorch time with faster sulfur vulcanization than NRF-TBBS-B4 as can be seen in Figure 4.12 and 4.13. Furthermore, NRF-CBS-B4 and NRF-CBS2-B4 have the same cure characteristics even though they have slightly different quantity of CBS accelerator. It is obvious that NRF-CBS2-B4 shows different cure characteristics compared to NRF-TBBS-B4. This means that there is no significant effect of quantity of reactive site or accelerator to sulfur molar ratio in our natural rubber foam system.

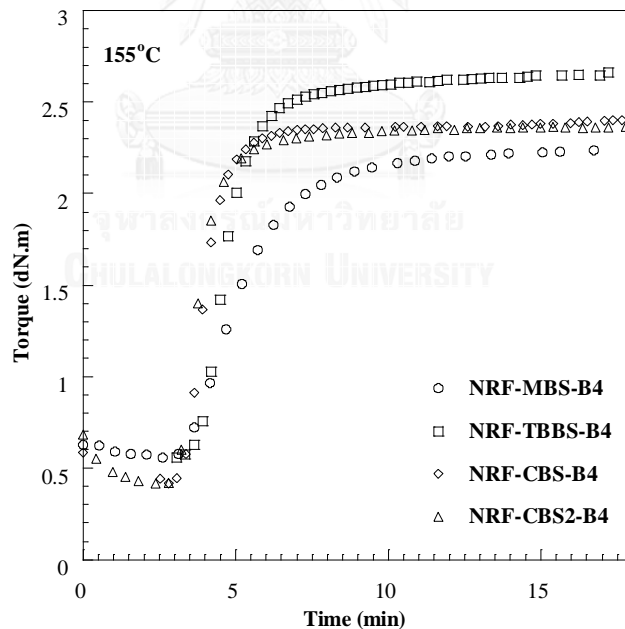


Figure 4.12 Torque measurement of natural rubber foam at 4 phr of chemical blowing agent produced at 155°C of processing temperature with different sulfenamide accelerators

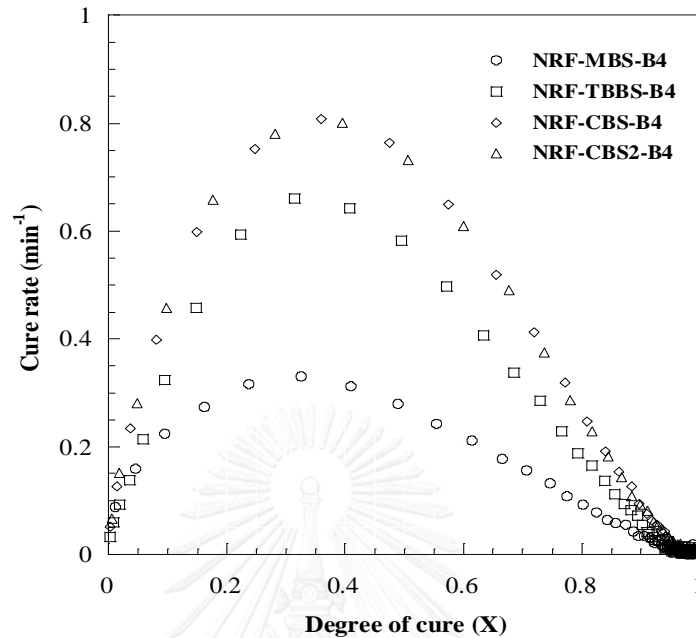


Figure 4.13 Cure characteristics of natural rubber foam at 4 phr of chemical blowing agent produced at 155°C of processing temperature with different sulfenamide accelerators

The degree of cure ( $X$ ) and cure rate ( $\frac{dX}{dt}$ ) of natural rubber foam with different types of sulfenamide accelerator were determined by various processing temperatures from 155 to 170°C. Figure 4.14 shows cure rate ( $\frac{dX}{dt}$ ) as a function of degree of cure ( $X$ ). The higher processing temperature is used, the faster sulfur vulcanization is obtained following Arrhenius's equation as discussed previously. The different type of sulfenamide accelerators cause different cure characteristics with

various processing temperatures. After that, they are fitted with autocatalytic equation using Matlab program as mentioned previously in section 4.1.1. The results of these fitted data and some important data from moving die rheograph are summarized in Table 4.2.

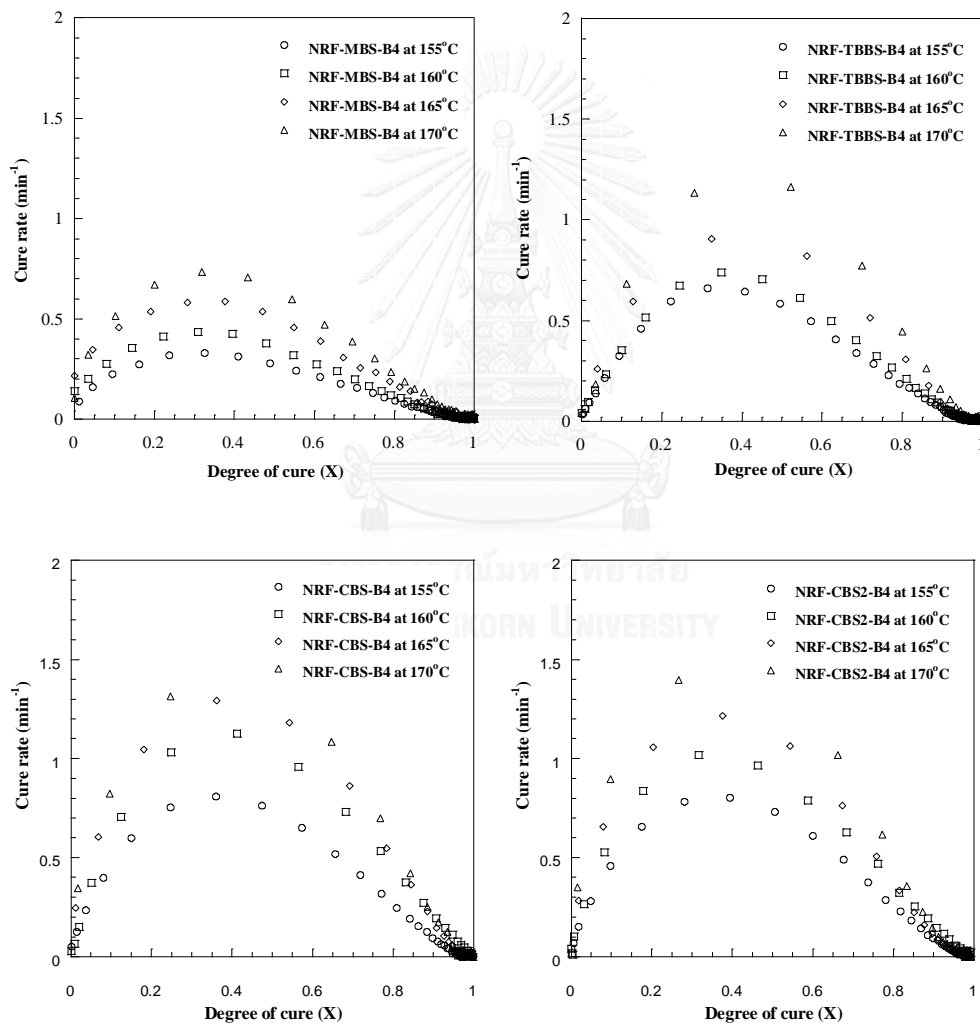


Figure 4.14 Cure characteristics of natural rubber foam at 4 phr of chemical blowing agent with different sulfenamide accelerators and processing temperature



Table 4.2 Summary of the cure kinetics and kinetic parameters of natural rubber foam at 4 phr of chemical blowing agent with different sulfenamide accelerators

Sample name	Acc:S (by mole)	$t_{s1}^*$ (min)	$t_{10}^*$ (min)	$t_{c90}^*$ (min)	n order	m order	K(T) (min <sup>-1</sup> )	$E_a$ (kJ/mol)
NRF-MBS-B4 at 155°C	5.08	5.39	3.90	8.48	1.46	0.62	1.15	83.41
NRF-MBS-B4 at 160°C	5.08	4.25	3.00	6.73	1.57	0.65	1.65	
NRF-MBS-B4 at 165°C	5.08	3.19	2.23	4.84	1.44	0.58	1.98	
NRF-MBS-B4 at 170°C	5.08	2.39	1.60	3.59	1.42	0.63	2.62	
NRF-TBBS-B4 at 155°C	5.38	4.58	4.06	6.40	1.79	0.97	3.95	66.90
NRF-TBBS-B4 at 160°C	5.38	3.90	3.28	5.41	1.72	0.99	4.34	
NRF-TBBS-B4 at 165°C	5.38	2.92	2.39	3.96	1.61	0.95	5.19	
NRF-TBBS-B4 at 170°C	5.38	2.27	1.81	2.96	1.62	1.05	7.57	
NRF-CBS-B4 at 155°C	4.85	4.01	3.50	4.98	1.46	0.81	3.88	54.19
NRF-CBS-B4 at 160°C	4.85	3.03	2.66	3.76	1.33	0.83	4.74	
NRF-CBS-B4 at 165°C	4.85	2.54	1.95	3.13	1.43	0.82	5.82	
NRF-CBS-B4 at 170°C	4.85	2.24	1.68	2.64	1.42	0.82	6.43	
NRF-CBS2-B4 at 155°C	5.38	3.79	3.21	5.06	1.57	0.85	3.89	64.49
NRF-CBS2-B4 at 160°C	5.38	3.05	2.53	3.87	1.41	0.79	4.30	
NRF-CBS2-B4 at 165°C	5.38	2.44	1.90	3.28	1.62	0.83	6.01	
NRF-CBS2-B4 at 170°C	5.38	1.97	1.53	2.56	1.54	0.81	6.88	

\* $t_{s1}$  = scorch time,  $t_{10}$  = time at 10% of torque increment,  $t_{c90}$  = cure time

The processing temperature does not affect  $n$  and  $m$  order of reaction but increasing processing temperature results in high cure rate constant ( $K$ ). This is following Arrhenius's equation. The increase of processing temperature refers to the increase of kinetic energy of our complex species; the forming molecules among activator, co-activator, accelerator and sulfur, to collide rubber molecules and forms three dimensional networks by sulfur. The highest  $m$  orders of reaction from NRF-TBBS-B4 means the highest crosslink network of natural rubber foam product in this section which is consistent with the obtained maximum torque from rheograph as can be seen in Figure 4.12. However, the highest crosslink density does not relate to the fastest sulfur vulcanization rate. Both NRF-CBS-B4 and NRF-CBS2-B4 show the lowest activation energy ( $E_a$ ) compared to other NRF product with other sulfenamide accelerators. Therefore, the natural rubber foam with CBS accelerator has the fastest sulfur vulcanization rate. The low activation energy in vulcanization means crosslink reaction by sulfur could be easily occurred. The cure time ( $t_{c90}$ ) in this section is used as time to compress rubber compound in the mold for producing natural rubber foam specimen. Morphology and other properties such as physical, mechanical and thermal properties are determined in the following section.

#### 4.2.2. Effect of sulfenamide accelerators on morphology of NRF product

The bubble diameter and microvoid structure of natural rubber foam (NRF) with different sulfenamide accelerators in cross-section fractured surface are observed in Figure 4.15. NRF-MBS-B4 shows different microvoid structure with large variation of size distribution. This is caused by the slowest sulfur vulcanization rate of NRF with MBS accelerator as discussed in section 4.2.1. The slowest sulfur vulcanization affecting long expansion time and diffusion time of gas bubbles in natural rubber matrix. Furthermore, microvoid structures of NRF-TBBS-B4, NRF-CBS-B4 and NRF-CBS2-B4 are not different because TBBS and CBS accelerator have slightly different acceleration rate as shown in Figure 4.13. Because of similar bubble diameter and microvoid structure of TBBS and CBS accelerator, the average bubble diameter and bubble size distribution in rubber foam product were analyzed by using SEM images and calculated by using arithmetic mean method [100].

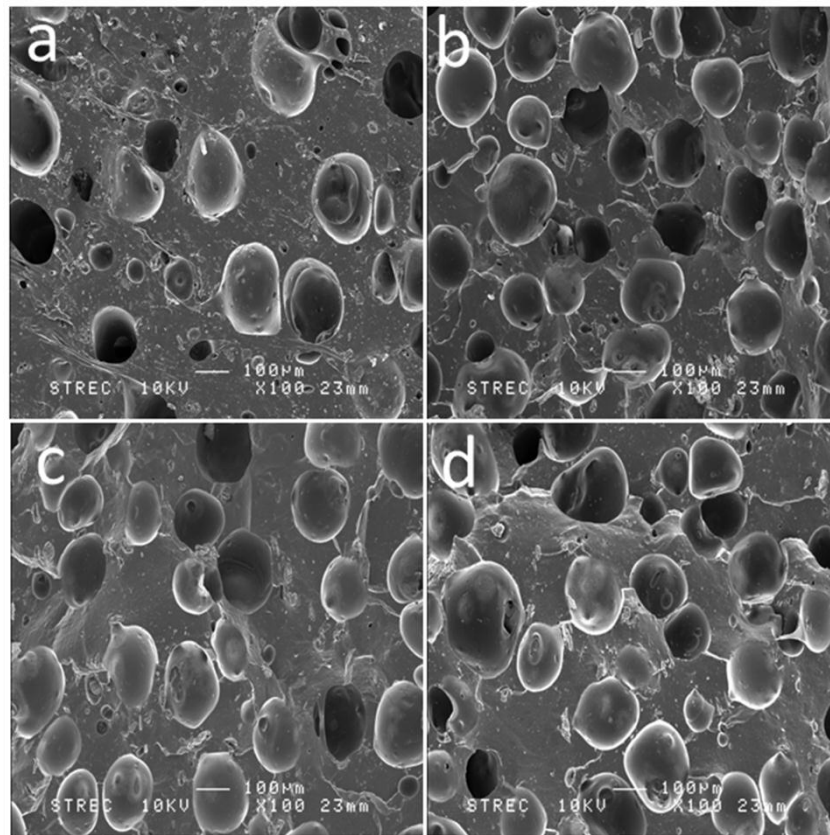


Figure 4.15 SEM images of natural rubber foam specimen at 4 phr of chemical blowing agent produced at 155°C of processing temperature (a) NRF-MBS-B4, (b) NRF-TBBS-B4, (c) NRF-CBS-B4 and (d) NRF-CBS2-B4

#### 4.2.3. Effect of sulfenamide accelerators on physical, mechanical and thermal properties of NRF product

The average ferret bubble diameter and bubble size distribution were calculated by collecting the data from 160 bubbles in each formulas. In Table 4.3, NRF-MBS-B4 contains the largest bubble diameter with the broadest size distribution

due to the slowest sulfur vulcanization rate. In case of NRF-CBS-B4 and NRF-CBS2-B4, they show similar bubble diameter due to the same sulfur vulcanization rate. For NRF-TBBS-B4, it has slightly larger bubble diameter than rubber foam with CBS accelerator systems owing to slightly lower sulfur vulcanization rate. It could be concluded that bubble diameter and size distribution of NRF can be controlled by adjusting sulfur vulcanization rate because the fast sulfur vulcanization induces small bubble diameter with narrow size distribution from the limit of gas expansion during foam formation. Bulk density and skeleton density (the density of rubber without air bubbles) of NRF in this section were measured and used to calculate the cell density with average bubble mean diameter from SEM analysis. The result is also shown in Table 4.3. Bulk densities of rubber foam produced at 155°C do not change with different sulfenamide accelerators, suggesting that the amount of air trapped inside the sample is constant. Although NRF-MBS-B4 shows different microvoid structures from other sulfenamide accelerator systems as seen by SEM images in Figure 4.15, the largest bubble diameter with broadest size distribution caused by the slowest sulfur vulcanization are obtained. These results explain why NRF-MBS-B4, which exhibits thicker microvoid structure than other NRF with other sulfenamide accelerators, has similar bulk density. Furthermore, NRF with CBS accelerator systems reveal the highest cell density owing to the fastest sulfur vulcanization.

Table 4.3 Physical properties of NRF with different sulfenamide accelerators

Sample name	Bubble diameter ( $\mu\text{m}$ )	Bulk density ( $\text{g}/\text{cm}^3$ )	Skeleton density ( $\text{g}/\text{cm}^3$ )	Cell density ( $\text{Cells}/\text{cm}^3$ )
NRF-MBS-B4	172 $\pm$ 2.43	0.680 $\pm$ 0.010	0.822 $\pm$ 0.026	6.40 $\times 10^4$
NRF-TBBS-B4	167 $\pm$ 2.39	0.682 $\pm$ 0.006	0.814 $\pm$ 0.018	6.62 $\times 10^4$
NRF-CBS-B4	164 $\pm$ 2.10	0.671 $\pm$ 0.002	0.812 $\pm$ 0.013	7.37 $\times 10^4$
NRF-CBS2-B4	165 $\pm$ 2.09	0.681 $\pm$ 0.003	0.836 $\pm$ 0.005	7.81 $\times 10^4$

The compression set of NRF with different sulfenamide accelerators was measured to investigate how NRF product could retain the original shape after removing the applied compressive stress. The compression set was tested following ASTM D395 method B under 70°C of aging temperature for 22 hours. In Figure 4.16, NRF-MBS-B4 and NRF-TBBS-B4 show slightly lower percentage of compression set than NRF with CBS accelerators. The low percentage of compression set refers to high ability of specimen to maintain the original shape after removing compressive stress. NRF-MBS-B4 has low percentage of compression set as a result of thick microvoid structure. Although NRF with CBS and TBBS accelerator systems have similar microvoid structure, NRF-CBS-B4 and NRF-CBS2-B4 have higher percentage of compression set than NRF-TBBS-B4 because they have high cell density which means high amount of gas bubbles per unit volume of NRF specimen. The higher volume of

gas bubbles contain in specimen, the weaker of microvoid structure could be obtained thus; these rubber foam systems could not retain the original shape after releasing the compressive stress.

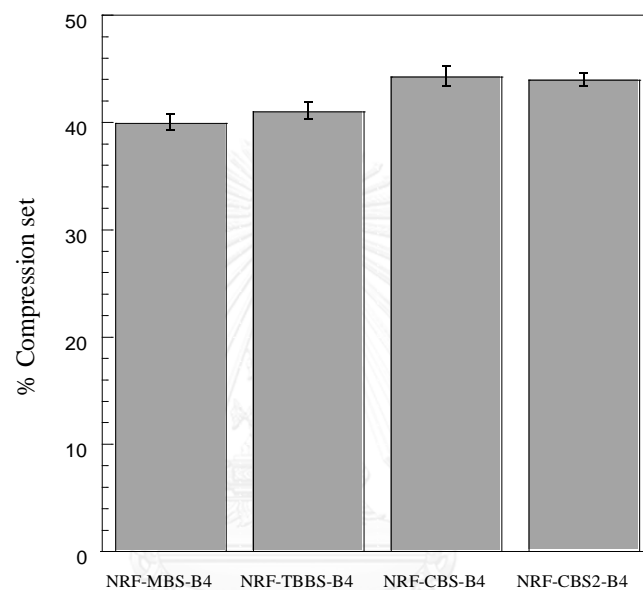
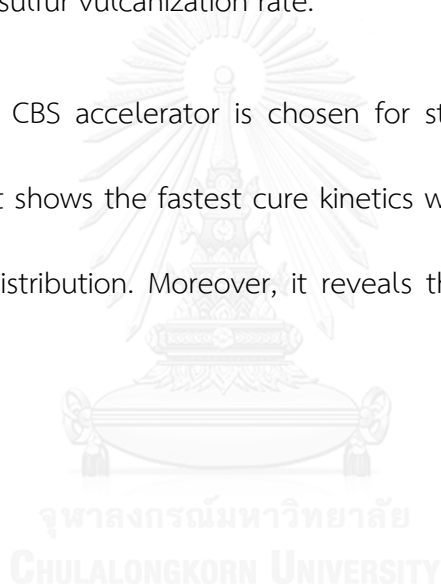


Figure 4.16 Percentage of compression set of natural rubber foam at 4 phr of chemical blowing agent with different sulfenamide accelerators produced at 155°C of processing temperature

Another property that should be concerned in this section is thermal properties including thermal expansion coefficient and thermal conductivity of specimen. From Figure 4.17, NRF-CBS-B4 and NRF-CBS2-B4 show the lowest thermal expansion coefficient compared to NRF-MBS-B4 and NRF-TBBS-B4. This is because

NRF with CBS accelerator systems have small sized bubbles with narrow size distribution caused by the fastest sulfur vulcanization rate. Moreover, from Figure 4.18, thermal conductivity of the specimen with different sulfenamide accelerators slightly change due to the same gas volume in rubber matrix of all formulas which is consistent with the bulk density of NRF. NRF-CBS-B4 and NRF-CBS2-B4 have slightly lower thermal conductivity than NRF-TBBS-B4 and NRF-MBS-B4 due to high cell density from the fast sulfur vulcanization rate.

The NRF with CBS accelerator is chosen for studying the effect of filler in section 4.3 because it shows the fastest cure kinetics with smallest bubble diameter and narrowest size distribution. Moreover, it reveals the lowest thermal expansion coefficient.





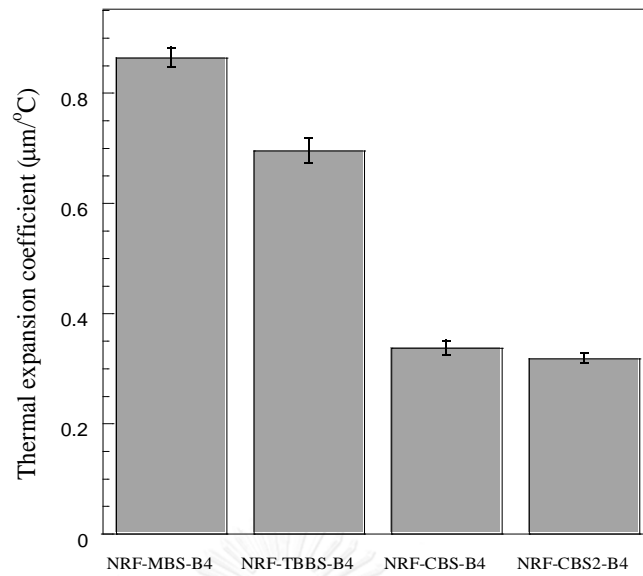


Figure 4.17 Thermal expansion coefficient of natural rubber foam at 4 phr of chemical blowing agent with different sulfenamide accelerators produced at 155°C of processing temperature

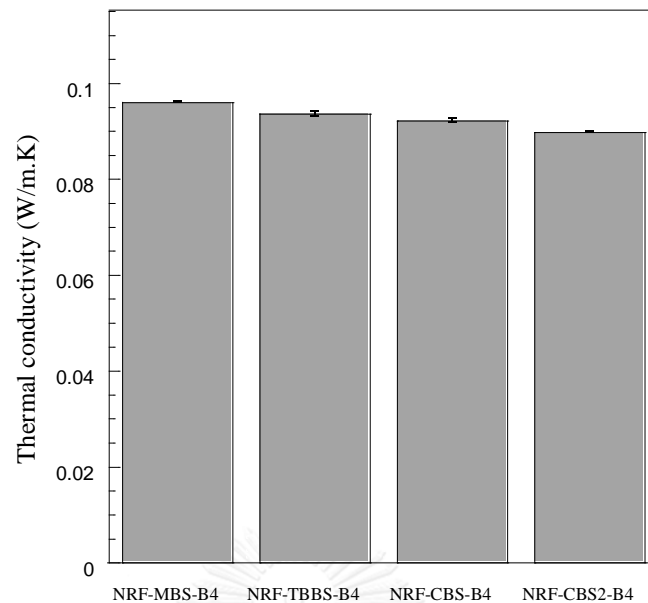


Figure 4.18 Thermal conductivity of natural rubber foam at 4 phr of chemical blowing agent with different sulfenamide accelerator produced at 155°C of processing temperature

### 4.3. Effect of graphene and surface treatment of graphene on cure characteristics and properties of natural rubber foam

#### 4.3.1. Surface chemistry of graphene

Graphene is used as filler in this research because it has excellent mechanical and thermal properties. Some researchers also supported that it could improve mechanical properties of elastomer nanocomposites better than other carbon materials as discussed in literature [52, 72, 73]. However, there is no research of NR/graphene nanocomposite foam which is different from using graphene as filler in

vulcanized natural rubber without foam. In rubber foam system, filler affects not only mechanical properties of material from reinforcing effect, but also foam formation mechanism resulting in different microvoid structures. Our research focuses on the effect of graphene on sulfur vulcanization rate of NR/graphene nanocomposite foam. It has been found in previous section that the different sulfur vulcanization rate shows different properties of natural rubber foam (NRF) due to different microvoid structure. Moreover, Wu et al. [65] reported that graphene accelerated sulfur vulcanization from its remaining oxygen functional groups which might change the microvoid structure in NR/graphene nanocomposite foam. However, the aggregation of graphene in rubber matrix might reduce the performance of graphene when it was mixed with natural rubber. This problem can be solved by treating the surface of graphene. In this section, the functional groups of surface treated graphene with cyclohexyl diamine and untreated graphene are investigated and the possible mechanism of surface treated graphene from our method is proposed to understand how cyclohexyl diamine is attached on the surface of graphene. The functional group of untreated graphene (UG) and treated graphene with cyclohexyl diamine (CG) were analyzed by Fourier Transform Infrared spectroscopy (FTIR) as seen in Figure 4.19. Graphene without surface treatment (UG) has remaining oxygen functional groups on its surface. The broad peak around 3000-3400  $\text{cm}^{-1}$  of untreated graphene refers to hydroxyl group. The peak around 1500-1700  $\text{cm}^{-1}$  refers to carboxylic group. The epoxide group on surface of graphene can

be detected at 1200 and 1380  $\text{cm}^{-1}$  of FTIR spectrum. The remaining oxygen functional groups on surface of graphene may be caused by the incomplete reduction of oxygen functional groups during graphene synthesis from the supplier. After graphene was treated with cyclohexyl diamine via diazonium reaction (CG), the peak of remaining oxygen functional groups are still observed and the new peak around 2800-2900  $\text{cm}^{-1}$  which is the  $\text{CH}_2\text{-CH}_2$  bond from cyclohexyl structure is observed. This might be due to the chemical linkage of cyclohexyl on the surface of graphene via free radical addition of diazonium salt mechanism.

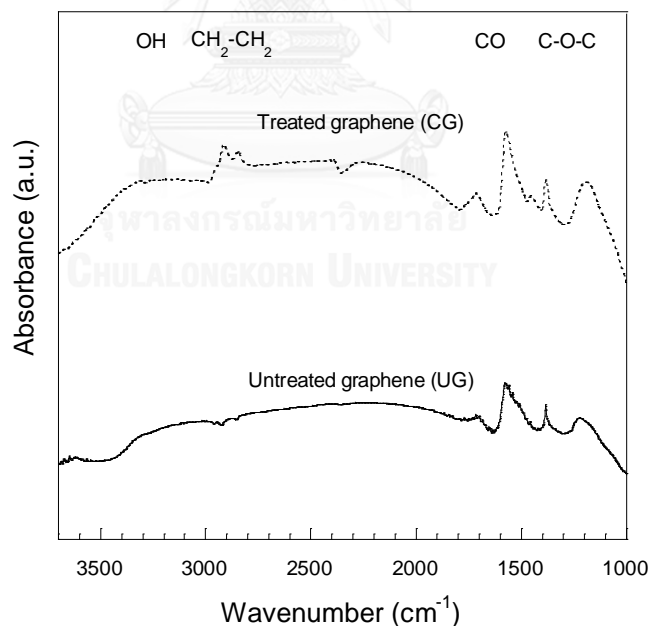


Figure 4.19 FTIR spectrum of untreated graphene (UG) and treated surface of graphene by cyclohexyl diamine (CG)

Raman spectrum of graphene nanoplatelet is studied to analyze the defects on the surface of graphene as shown in Figure 4.20. The G and D peaks of Raman spectrum refer to the perfect structure of carbon in hexagonal honeycomb structure and the defect or imperfect structure of carbon from synthesis respectively. It has been found that the Raman peaks of treated graphene (CG) are slightly shifted from those of untreated graphene (UG) around 1341 and 1570  $\text{cm}^{-1}$  to 1338 and 1569  $\text{cm}^{-1}$  of D and G peak respectively. The intensity ratio of D to G ( $I_D/I_G$ ) of treated graphene is higher than that of untreated graphene referring to more defect molecules on the graphene surface. This might be due to molecular attraction of cyclohexyl diamine on surface of graphene.

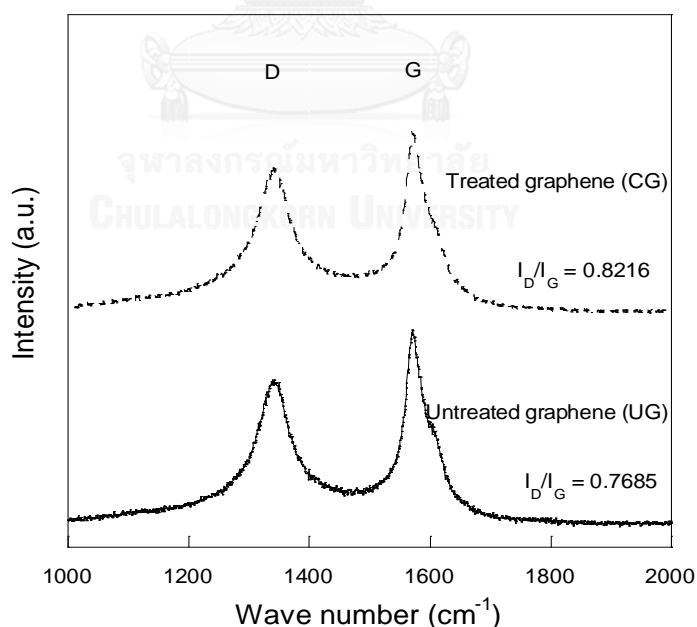


Figure 4.20 Raman spectrum of untreated graphene (UG) and treated surface of graphene by cyclohexyl diamine (CG)

Thermal decomposition of graphene nanoplatelet was tested to confirm the surface functional groups of graphene treated with cyclohexyl diamine. It has been found from Figure 4.21 that treated graphene (CG) has lower thermal stability than untreated graphene (UG) due to the thermal decomposition of cyclohexyl diamine and the increase of oxygen functional group on the surface of graphene from surface treatment process in which the weight of CG decreases dramatically at 200-250°C. This could be confirmed that surface treated graphene (CG) has more defect molecules on the surface than untreated graphene (UG) from the treatment process.

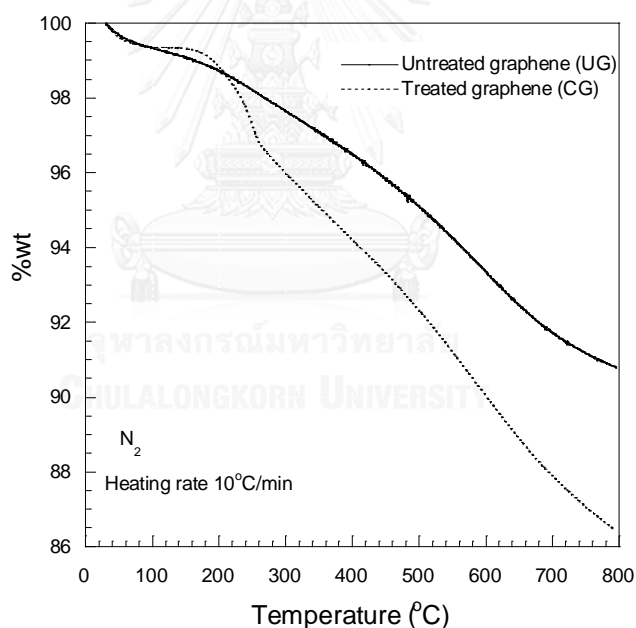


Figure 4.21 Thermal decomposition of untreated graphene (UG) and treated surface of graphene by cyclohexyl diamine (CG)

The possible mechanism of surface treatment of graphene based on the free radical addition of diazonium salt mechanism [76, 80, 98, 99] is proposed in Figure 4.22 to explain how the cyclohexyl diamine can attach on the surface of graphene. The mechanism begins with sodium nitrite reacts with sulfuric acid to form nitrogen dioxide and nitric oxide radicals. Next, they react with amine in cyclohexyl diamine structure to form diazonium cation and rearrange to cyclohexyl radicals. The cyclohexyl radical reacts on the graphene surface to form modified graphene with cyclohexyl amine group or treated graphene (CG).

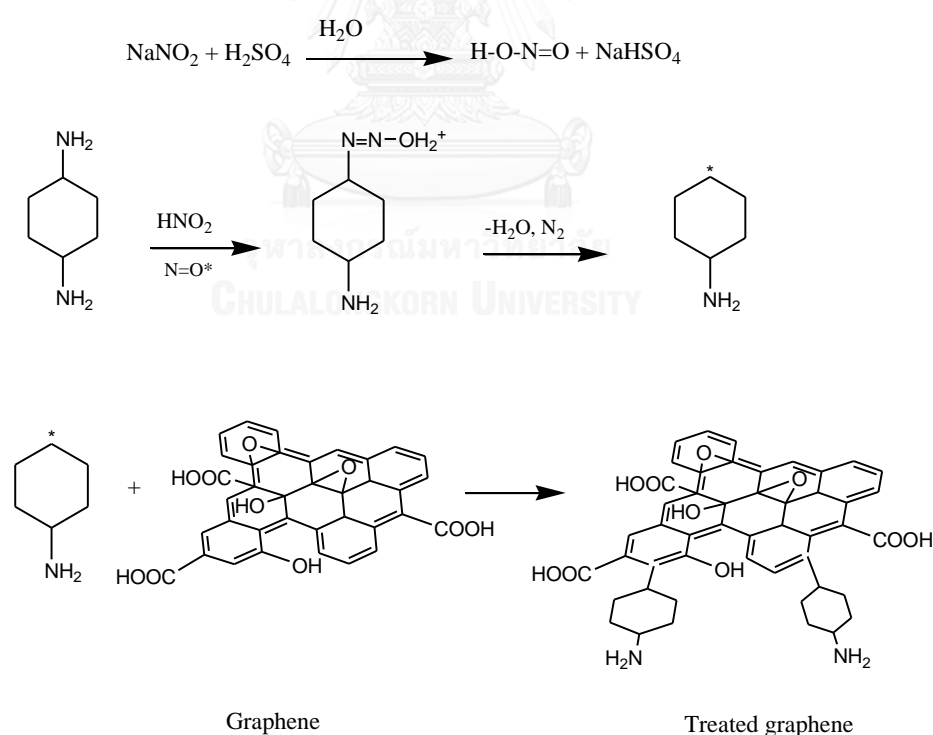


Figure 4.22 Possible mechanism of surface treatment of graphene by cyclohexyl diamine via diazonium reaction

#### 4.3.2. Cure characteristics of NR/graphene nanocomposite foam

The chemical blowing agent of natural rubber compound in this section was fixed at 5 phr because the different source of chemicals in sulfur vulcanization from those in the previous section. It was observed from SEM images that adding 5 phr of new batch of azodicarbonamide in rubber compound showed more uniform with non-coalescence of bubbles in rubber matrix. Besides the change in chemical blowing agent content, the composition of other chemicals in sulfur vulcanization is similar to those in the previous section. The effect of untreated graphene content on cure characteristic is studied in the range of 0-3 phr. The addition of surface treated graphene with cyclohexyl diamine at 3 phr of graphene content in NRF is also investigated. In this part, only cure characteristics of natural rubber compound at 155°C is presented owing to the small amount of synthesized graphene with cyclohexyl diamine from diazonium reaction. The torque measurement of NR/graphene nanocomposite foam containing untreated graphene (UG) and treated graphene (CG) is shown in Figure 4.23. It has been found that the shortest scorch time is obtained at 2 and 3 phr of untreated graphene in NR/graphene nanocomposite foam. The untreated graphene is limited at 3 phr due to the same cure characteristics of nanocomposite foam compared to that with 2 phr of untreated graphene. The presence of untreated graphene accelerates sulfur vulcanization rate due to the remaining oxygen functional groups on the surface of



graphene which is consistent with work from Wu et al. [65]. They explained that hydroxyl and carboxylic groups on the surface of graphene could react with sulfur vulcanizing agent to form thiol, thioester, and dithiocarboxylic ester groups which also formed sulfurating species similar to sulfenamide accelerators. These molecules can attract rubber molecules to form crosslink network by sulfur. Moreover, NR/graphene nanocomposite foam with treated surface of graphene (CG) shows slower sulfur vulcanization rate than that with untreated graphene (UG) at the same composition. This might be the reaction between amine from cyclohexyl diamine and the remaining oxygen functional groups on the graphene surface, reducing the amount of oxygen-containing groups that could react with sulfur vulcanization agent to form reactive sulfurating species. Another reason is that the steric hindrance of cyclohexyl group might retard sulfur vulcanization from obstruction of crosslinking network by sulfur. The results of cure rate with different untreated graphene content and surface treated graphene are observed in Figure 4.24. The trend of cure rate of NR/graphene nanocomposite foam while varying graphene content is similar to the torque measurement as discussed previously. Namely, cure rate increases as the untreated graphene increases in NR/graphene nanocomposite foam. Moreover, NRF-CBS-B5-CG3 shows the lowest sulfur vulcanization rate.

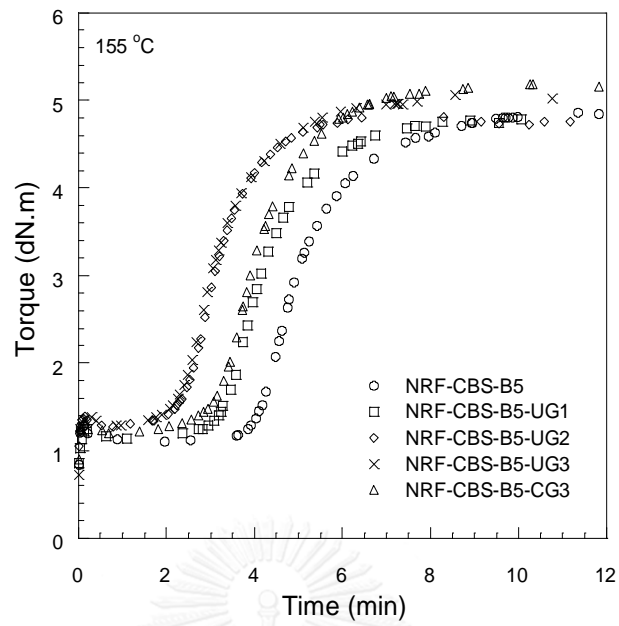


Figure 4.23 Torque measurement of NRF at 155°C with untreated graphene (UG) and treated surface of graphene (CG)

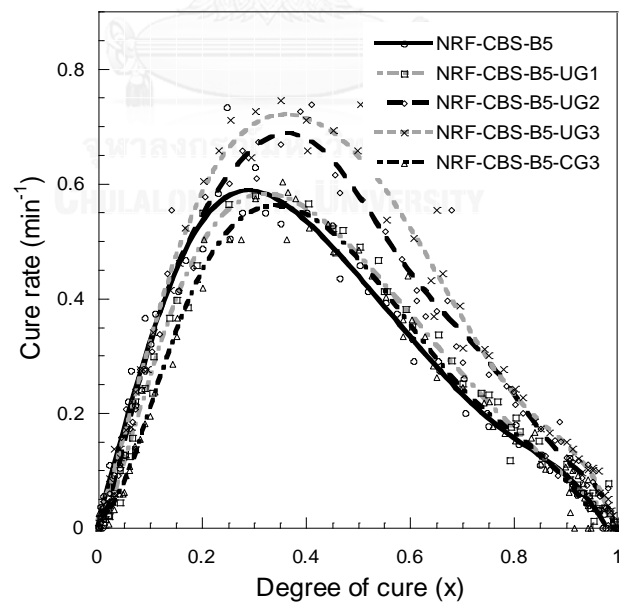


Figure 4.24 Cure characteristics of NRF at 155°C with untreated graphene (UG) and treated surface of graphene (CG)

#### 4.3.3. Morphology of graphene/natural rubber foam nanocomposites

It should be noted that the effect of surface functionality of graphene on the dispersion of graphene in rubber matrix was observed from vulcanized natural rubber without the addition of chemical blowing agent because it is difficult to observe the dispersion of graphene in the foam by transmission electron microscopy. The degree of dispersion of graphene particle in vulcanized natural rubber without chemical blowing agent at 3 phr of untreated graphene (UG) and treated graphene (CG) are investigated. This is the important factor for improving mechanical properties when graphene is remained in natural rubber foam specimen. Figure 4.25 reveals that untreated graphene without (UG) aggregates in the rubber matrix while surface treated graphene (CG) shows better dispersion in rubber matrix due to the hindrance effect of cyclohexyl molecules on the graphene's surface.

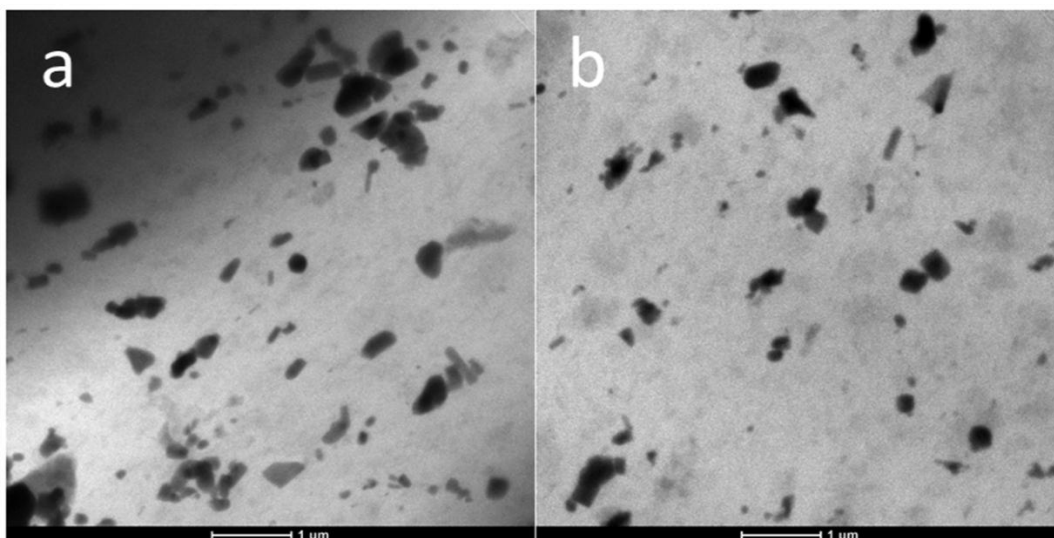


Figure 4.25 TEM images of vulcanized natural rubber at 3 phr of untreated graphene (a) and surface treated graphene with cyclohexyl diamine (b)

Morphology of NR/graphene nanocomposite foam at different untreated graphene content and surface functionality of graphene was observed by scanning electron microscopy as seen in Figure 4.26. The bubble diameter and microvoid structure of nanocomposite foam directly relate to cure characteristics of their systems as discussed in the previous section. NRF-CBS-B5-UG3 shows the smallest bubble diameter caused by the fastest sulfur vulcanization rate. Furthermore, NRF-CBS-B5-CG3 which has the slowest sulfur vulcanization rate shows smaller bubble diameter than NRF-CBS-B5, NRF-CBS-B5-UG1 and NRF-CBS-B5-UG2 because the bubble growth is limited by high filler content and defect molecules of cyclohexyl diamine on the graphene surface. In addition, NRF-CBS-B5-CG3 has larger bubble

diameter than NRF-CBS-B5-UG3 due to slow sulfur vulcanization rate. This might be concluded that not only the sulfur vulcanization rate but the filler content and functional groups on the graphene surface also affect the bubble growth in natural rubber matrix. Thus these effects should be concerned simultaneously.

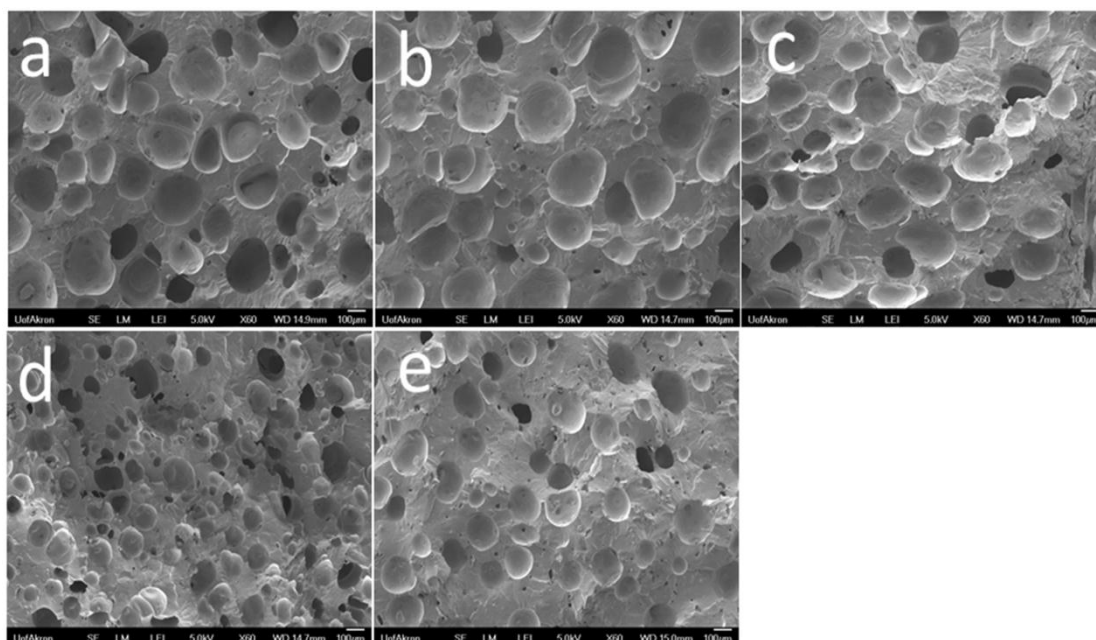


Figure 4.26 SEM images of (a) NRF-CBS-B5, (b) NRF-CBS-B5-UG1, (c) NRF-CBS-B5-UG2, (d) NRF-CBS-B5-UG3, (e) NRF-CBS-B5-CG3

#### 4.3.4. Physical, mechanical and thermal properties of NR/graphene nanocomposite foam

The bubble diameter and size distribution of natural rubber foam (NRF) while varying untreated graphene contents and with treated graphene at 3 phr are calculated from 230 bubbles per each formula by using SEM images. It has been found from Table 4.4 that the increase of untreated graphene content reduces bubble diameter with narrow size distribution. In addition, the nanocomposite foam with treated surface of graphene contains slightly large bubble diameter with the narrowest size distribution. Table 4.4 also shows the bulk density and skeleton density. They were used to calculate cell density with bubble diameter similar to section 4.2. Cell density increases with the presence of untreated graphene because the porosity does not change due to the similar trend of increment of bulk density and skeleton density but the mean bubble diameter in the rubber matrix reduces with increasing graphene content. Furthermore, NRF-CBS-B5-CG3 shows the lowest

cell density due to high content of treated graphene combined with the slowest sulfur vulcanization rate in which the bubble growth is limited.

Table 4.4 Physical properties of NRF with and without untreated graphene (UG) and surface treated graphene with cyclohexyl diamine (CG)

Sample name	Bubble diameter ( $\mu\text{m}$ )	Bulk density ( $\text{g}/\text{cm}^3$ )	Skeleton density ( $\text{g}/\text{cm}^3$ )	Cell density ( $\text{cells}/\text{cm}^3$ )
NRF-CBS-B5	252 $\pm$ 2.77	0.62 $\pm$ 0.0021	0.76 $\pm$ 0.0041	2.23 $\times 10^4$
NRF-CBS-B5-UG1	196 $\pm$ 2.14	0.65 $\pm$ 0.0051	0.78 $\pm$ 0.0039	4.13 $\times 10^4$
NRF-CBS-B5-UG2	202 $\pm$ 1.63	0.67 $\pm$ 0.0040	0.80 $\pm$ 0.0056	4.15 $\times 10^4$
NRF-CBS-B5-UG3	162 $\pm$ 1.54	0.66 $\pm$ 0.0132	0.80 $\pm$ 0.0041	7.86 $\times 10^4$
NRF-CBS-B5-CG3	172 $\pm$ 1.24	0.76 $\pm$ 0.0170	0.80 $\pm$ 0.0036	2.06 $\times 10^4$

The tensile properties and compression set of NR/graphene nanocomposite foam with different untreated graphene contents and treated graphene are shown in

Table 4.5. Tensile strength at break of nanocomposite foam increases with the

presence of untreated graphene because graphene can reinforce the rubber nanocomposites by improving the load transfer at the interface. For NRF-CBS-B5-UG2 and NRF-CBS-B5-UG3, the tensile strengths are not different. Although NRF-CBS-B5-UG3 has higher graphene content than NRF-B5-UG2, it shows the highest cell density per unit volume with small bubble size resulting in weakness of microvoid structure.

On the other hand, the presence of 3 phr of treated graphene in NRF-CBS-B5-CG3 increases tensile strength at break around 68 % compared to NRF-CBS-B5. This might be due to the lowest cell density and better dispersion of graphene in natural rubber foam as can be supported by data in Table 4.4 and TEM images. Moreover, the elongation at break of nanocomposite foam increases when adding graphene in NR/graphene nanocomposite foam and slightly reduces with increasing graphene content. However, the elongation at break of NRF-CBS-B5-CG3 does not lower than that of NRF without graphene. In addition, the percentage of compression set of NRF-CBS-B5-UG3 is slightly lower than that of other NR/graphene nanocomposite foam systems due to the smallest bubble diameter of this formula which can distribute the compressive stress and retain the shape of specimen during testing effectively.



Table 4.5 Mechanical properties of NRF with and without untreated graphene (UG) and surface treated graphene with cyclohexyl diamine (CG)

Sample name	Tensile strength at break (MPa)	Elongation at break (%)	Compression set (%)
NRF-CBS-B5	7.22±0.34	597±16.27	30.00±0.70
NRF-CBS-B5-UG1	8.30±0.48	661±30.51	31.80±1.60
NRF-CBS-B5-UG2	9.55±0.47	616±25.59	32.80±1.60
NRF-CBS-B5-UG3	9.45±0.29	605±29.08	28.30±1.70
NRF-CBS-B5-CG3	12.12±0.43	609±31.06	30.60±1.70

Thermal properties of NR/graphene nanocomposite foam in this section including thermal expansion coefficient and thermal conductivity are displayed in Table 4.6. Thermal expansion coefficient of NRF-CBS-B5, NRF-CBS-B5-UG1 and NRF-CBS-B5-UG2 is similar. The small bubble diameter of NRF-CBS-B5-UG3 and NRF-CBS-B5-CG3 cause lower thermal expansion coefficient than the system without graphene

in rubber matrix. It has been found that NRF-CBS-B5-CG3 displays the lowest thermal expansion coefficient. This is caused by small bubble diameter with the lowest cell density in rubber matrix. The thermal conductivity of NR/graphene nanocomposite foam slightly increases with the presence of untreated graphene due to the high thermal conductivity of pristine graphene. However, it does not increase much because of low filler content and the effect of bubble inside rubber matrix. In addition, thermal conductivity of NRF-CBS-B5-CG3 is slightly lower than that of NRF-CBS-B5-UG3. This might be owing to more defects on surface of graphene during surface modification via diazonium process with high acidic condition during surface treatment process [101-103].

Table 4.6 Thermal properties of NRF with and without untreated graphene (UG) and surface treatment of graphene with cyclohexyl diamine (CG)

Sample name	Thermal expansion coefficient ( $\mu\text{m}/^\circ\text{C}$ )	Thermal conductivity (W/m.K)
NRF-CBS-B5	$0.69 \pm 0.099$	$0.062 \pm 0.001$
NRF-CBS-B5-UG1	$0.72 \pm 0.012$	$0.078 \pm 0.001$
NRF-CBS-B5-UG2	$0.74 \pm 0.053$	$0.078 \pm 0.004$
NRF-CBS-B5-UG3	$0.61 \pm 0.095$	$0.074 \pm 0.001$
NRF-CBS-B5-CG3	$0.49 \pm 0.007$	$0.066 \pm 0.001$

## CHAPTER V

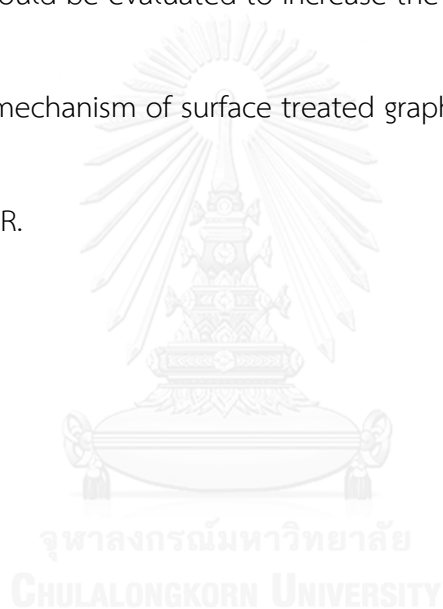
### CONCLUSIONS AND RECOMMENDATION

The development of natural rubber foam (NRF) in this research mainly focuses on the influence of chemical ingredients in natural rubber foam and natural rubber nanocomposite foam on the sulfur vulcanization, morphology and other properties including mechanical and thermal properties. The presence of chemical blowing agent is investigated in the first part followed by the different sulfenamide accelerators and the amount of untreated graphene and surface treated graphene with cyclohexyl diamine via diazonium reaction. To answer our research question about how to control the size of NRF specimen with good mechanical and thermal properties, this problem depends on how much of gas could be preserved in rubber matrix. The presence of azodicarbonamide should be optimized around 4-5 phr depending on grades of chemicals in sulfur vulcanizing agent. The N-cyclohexyl benzothiazole-2-sulfenamide or CBS accelerator is the suitable sulfenamide accelerator to control the growth of gas bubble in rubber matrix with good

properties of NRF specimen due to the fastest sulfur vulcanization rate among other sulfenamide accelerators. Moreover, natural rubber/graphene nanocomposite foam in which graphene is surface treated by cyclohexyl diamine exhibits the highest tensile strength at break with low cell density and good thermal properties. It could be concluded that natural rubber/graphene nanocomposite foam with 3 phr of surface treated graphene is the optimal one in this research because it shows small bubble diameter with low cell density resulting in low gas volume in rubber matrix while it exhibits high tensile properties with low thermal expansion coefficient which is appropriate for producing natural rubber foam to be used in automotive industries or advance industrial applications.

## Recommendation

1. Other accelerators in sulfur vulcanization system such as thiazole and sulfenimide should be explored.
2. The system of secondary accelerator when using sulfenamide as primary accelerator should be evaluated to increase the sulfur vulcanization rate.
3. The possible mechanism of surface treated graphene should be confirmed by solid state NMR.



## REFERENCES

- [1] Coran, A.Y. Chemistry of the vulcanization and protection of elastomers: A review of the achievements. Journal of Applied Polymer Science 87 (2003): 24-30.
- [2] Landrock, A.H. Hand book of plastic foam : type, properties, manufacture and applications. New Jersey: Park Ridge, 1995.
- [3] Majumdar, S. Rubber mixing : a practical guide for rubber processing. Bangkok: Rubber industry academy, 2012.
- [4] Najib, N.N., Ariff, Z.M., Bakar, A.A., and Sipaut, C.S. Correlation between the acoustic and dynamic mechanical properties of natural rubber foam: Effect of foaming temperature. Materials and Design 32(2) (2011): 505-511.
- [5] Jo, J.O., Saha, P., Kim, N.G., Chang Ho, C., and Kim, J.K. Development of nanocomposite with epoxidized natural rubber and functionalized multiwalled carbon nanotubes for enhanced thermal conductivity and gas barrier property. Materials & Design 83 (2015): 777-785.
- [6] Le Gac, P.Y., Arhant, M., Davies, P., and Muhr, A. Fatigue behavior of natural rubber in marine environment: Comparison between air and sea water. Materials & Design 65 (2015): 462-467.
- [7] Rodgers, B. Rubber compounding : Chemistry and applications. New York: Marcel Dekker, Inc., 2004.

- [8] Chen, N. The Effects of Crosslinking on Foaming of EVA. Doctor of Philosophy, Department of Mechanical and Industrial Engineering University of Toronto, 2012.
- [9] Khang, T.H. and Ariff, Z.M. Vulcanization kinetics study of natural rubber compounds having different formulation variables. Journal of Thermal Analysis and Calorimetry 109(3) (2011): 1545-1553.
- [10] Wang, P.Y., Qian, H.L., Yu, H.P., and Chen, J. Study on kinetic of natural rubber vulcanization by using vulcameter. Journal of Applied Polymer Science 88(3) (2003): 680-684.
- [11] Garcia, A.M. Evaluation of scrap tire-derived porous rubber tubing as a green membrane for sustainable water filtration (ECOL-Mem process). Department of civil and environmental engineering University of South Florida, 2007.
- [12] Coran, A.Y. Chapter 7 - Vulcanization. in Mark, J.E., Erman, B., and Roland, C.M. (eds.), The Science and Technology of Rubber (Fourth Edition), pp. 337-381. Boston: Academic Press, 2013.
- [13] Alam, M.N., Mandal, S.K., and Debnath, S.C. Bis(N-benzyl piperazino) thiuram disulfide and dibenzothiazyl disulfide as synergistic safe accelerators in the vulcanization of natural rubber. Journal of Applied Polymer Science 126(6) (2012): 1830-1836.
- [14] Aprem, A.S., Joseph, K., Laxminarayanan, R., and Thomas, S. Physical, mechanical, and viscoelastic properties of natural rubber vulcanizates cured



- with new binary accelerator system. Journal of Applied Polymer Science 87(14) (2003): 2193-2203.
- [15] Aprem, A.S., Mathew, G., Joseph, K., and Thomas, S. New binary accelerator system for sulphur vulcanization of natural rubber. KGK-Kautschuk und Gummi Kunststoffe 52(9) (1999).
- [16] Banerjee, B. Thiuram vulcanization of natural rubber in the presence of amines - application of ESR technique to elucidate the mechanism of vulcanization. Kautschuk und Gummi, Kunststoffe 37(1) (1984): 21-24.
- [17] Choi, D., Abdul Kader, M., Cho, B.H., Huh, Y.I., and Nah, C. Vulcanization kinetics of nitrile rubber/layered clay nanocomposites. Journal of Applied Polymer Science 98(4) (2005): 1688-1696.
- [18] Ghosh, P., Katare, S., Patkar, P., Caruthers, J.M., Venkatasubramanian, V., and Walker, K.A. Sulfur vulcanization of natural rubber for benzothiazole accelerated formulations: From reaction mechanisms to a rational kinetic model. Rubber Chemistry and Technology 76(3) (2003): 592-693.
- [19] Travas-Sejdic, J., Jelencic, J., Bravar, M., and Fröbe, Z. Characterization of the natural rubber vulcanizates obtained by different accelerators. European Polymer Journal 32(12) (1996): 1395-1401.
- [20] Kamoun, M., Nassour, A., and Michael, N. The effect of novel binary accelerator system on properties of vulcanized natural rubber. Advances in Materials Science and Engineering 2009 (2009).

- [21] Mariano, R.M., Da Costa, H.M., Oliveira, M.R.L., Rubinger, M.M., and Visconte, L.Y. The behavior of dithiocarbamate derivative as safety accelerator of natural rubber compounds. Journal of Applied Polymer Science 110(4) (2008): 1938-1944.
- [22] Marykutty, C.V., Mathew, G., Mathew, E.J., and Thomas, S. Studies on Novel Binary Accelerator System in Sulfur Vulcanization of Natural Rubber. Journal of Applied Polymer Science 90(12) (2003): 3173-3182.
- [23] Reshmy, R., Thomas, K.K., and Sulekha, A. N-benzoyl-N'N'-disubstituted thioureas-A new binary accelerator system and its effect of nucleophilicity in sulfur vulcanization of natural rubber. Journal of Applied Polymer Science 124(2) (2011): 978-984.
- [24] Susamma, A.P. Studies on new binary accelerator systems in rubber vulcanization. doctor of philosophy, Polymer science and rubber technology Cochin university of science and technology, 2002.
- [25] Susamma, A.P., Elizabeth Mini, V.T., and Kuriakose, A.P. Studies on novel binary accelerator system in sulfur vulcanization of natural rubber. Journal of Applied Polymer Science 79(1) (2001): 1-8.
- [26] Thomas, S.P. and Ettolil, M.J. Investigation on Synergic Activity of N-Benzylimine Aminothioformamide Binary Accelerator System in Sulfur Vulcanization of Natural Rubber. Journal of Applied Polymer Science 116(5) (2010): 2976-2981.

- [27] Aprem, A.S., Joseph, K., Mathew, T., Altstaedt, V., and Thomas, S. Studies on accelerated sulphur vulcanization of natural rubber using 1-phenyl-2, 4-dithiobiuret/tertiary butyl benzothiazole sulphenamide. European Polymer Journal 39(7) (2003): 1451-1460.
- [28] Datta, R.N., Debnath, S.C., and Noordermeer, J.M. Cure Modification of Natural Rubber Containing Benzothiazole Accelerators by Some Modified Thiocarbamyl Sulfenamides. Journal of Applied Polymer Science 90(14) (2003): 3835-3847.
- [29] Sae-oui, P., Sirisinha, C., Thepsuwan, U., and Thapthong, P. Influence of accelerator type on properties of NR/EPDM blends. Polymer Testing 26(8) (2007): 1062-1067.
- [30] Sung Min Kim, Chae Seok Nam, and Kim, K.J. TMTD, MBTS, and CBS Accelerator Effects on a Silica Filled Natural Rubber Compound upon Vulcanization Properties. Applied Chemistry for Engineering 22(2) (2011): 144-148.
- [31] Ahmadi, M. and Shojaei, A. Cure kinetic and network structure of NR/SBR composites reinforced by multiwalled carbon nanotube and carbon blacks. Thermochimica Acta 566 (2013): 238-248.
- [32] Konar, B.B. and Saha, M. Influence of polymer coated CaCO<sub>3</sub> on vulcanization kinetics of natural rubber/sulfur/N-oxydiethyl benzthiazyl

- sulfenamide (BSM) system. Journal of Macromolecular Science Pure and Applied Chemistry 49(3) (2012): 214-226.
- [33] Tang, M., Xing, W., Wu, J., Huang, G., Li, H., and Wu, S. Vulcanization kinetics of graphene/styrene butadiene rubber nanocomposites. Chinese Journal of Polymer Science 32(5) (2014): 658-666.
- [34] Wimolmala, E., Khongnual, K., and Sombatsompop, N. Mechanical and morphological properties of cellular NR/SBR vulcanizates under thermal and weathering ageing. Journal of Applied Polymer Science 114(5) (2009): 2816-2827.
- [35] Najib, N.N., Ariff, Z.M., Manan, N.A., Bakar, A.A., and Sipaut, C.S. Effect of blowing agent concentration on cell morphology and impact properties of natural rubber foam. Journal of Physical Science 20(1) (2009): 13-25.
- [36] Lee, E.K. and Choi, S.Y. Preparation and characterization of natural rubber foams: Effects of foaming temperature and carbon black content. Korean Journal of Chemical Engineering 24(6) (2007): 1070-1075.
- [37] Tangboriboon, N., Samattai, S., Kamonsawas, J., and Sirivat, A. Processing of kaolinite and alumina loaded in natural rubber composite foams. Materials and Manufacturing Processes 30(5) (2015): 595-604.
- [38] Wang, X., Feng, N., and Chang, S. Effect of precured degrees on morphology, thermal, and mechanical properties of BR/SBR/NR foams. Polymer Composites 34(6) (2013): 849-859.

- [39] Yamsaengsung, W. and Sombatsompop, N. Effect of chemical blowing agent on cell structure and mechanical properties of EPDM foam, and peel strength and thermal conductivity of wood/NR composite–EPDM foam laminates. Composites Part B: Engineering 40(7) (2009): 594-600.
- [40] Bhatti, A.S., Dollimore, D., Goddard, R.J., and O'Donnell, G. The effects of additives on the thermal decomposition of azodicarbonamide. Thermochimica Acta 76(3) (1984): 273-286.
- [41] Levai, G., Nyitrai, Z., and Meszlényi, G. Kinetics and mechanism of the thermal decomposition of azodicarbonamide, I. ACH - Models in Chemistry 135(6) (1998): 885-900.
- [42] Robledo-Ortiz, J.R., Zepeda, C., Gomez, C., Rodrigue, D., and González-Núñez, R. Non-isothermal decomposition kinetics of azodicarbonamide in high density polyethylene using a capillary rheometer. Polymer Testing 27(6) (2008): 730-735.
- [43] Pechurai, W., Muansupan, T., and Seawlee, P. Effect of foaming temperature and blowing agent content on cure characteristics, mechanical and morphological properties of natural rubber foams. Advanced Materials Research 844 (2014): 454-457.
- [44] Sombatsompop, N. and Lertkamolsin, P. Effects of chemical blowing agents on swelling properties of expanded elastomers. Journal of Elastomers and Plastics 32(4) (2000): 311-328.

- [45] Tangboriboon, N., Rortchanakarn, S., Petcharoen, K., and Sirivat, A. Effects of foaming agents and calcium carbonate on thermo-mechanical properties of natural rubber foams. Polimeri 35(1) (2015): 10-17.
- [46] Bashir, M.A., Shahid, M., Alvi, R.A., and Yahya, A.G. Effect of carbon black on curing behavior, mechanical properties and viscoelastic behavior of natural sponge rubber-based nano-composites. Key Engineering Materials. 2012 (2012). 532-539.
- [47] Han, J., Zhang, Y., Wu, C., Xie, L., and Ma, Y. Wet sliding abrasion of natural rubber composites filled with carbon black at different applied loads. Journal of Macromolecular Science, Part B: Physics 54(4) (2015): 401-410.
- [48] Karabork, F. and Tipirdamaz, S.T. Influence of pyrolytic carbon black and pyrolytic oil made from used tires on the curing and (dynamic) mechanical properties of natural rubber (NR)/styrene-butadiene rubber (SBR) blends. Express Polymer Letters 10(1) (2016): 72-82.
- [49] Kim, J.H., Koh, J.S., Choi, K.C., Yoon, J.M., and Kim, S.Y. Effects of foaming temperature and carbon black content on the cure characteristics and mechanical properties of natural rubber foams. Journal of Industrial and Engineering Chemistry 13(2) (2007): 198-205.
- [50] Matchawet, S., Nakason, C., and Kaesaman, A. Electrical and mechanical properties of conductive carbon black filled epoxidized natural rubber. Advanced Materials Research. 2014 (2014). 255-258.

- [51] Lovell, R.J. and Young, P.A. Introduction to Polymers, London: CRC Press, 2011.
- [52] Fu, D.H., Zhan, Y.H., Yan, N., and Xia, H.S. A comparative investigation on strain induced crystallization for graphene and carbon nanotubes filled natural rubber composites. Express Polymer Letters 9(7) (2015): 597-607.
- [53] Hernández, M., Bernal, M.M., Verdejo, R., Ezquerro, T.A., and López-Manchado, M.A. Overall performance of natural rubber/graphene nanocomposites. Composites Science and Technology 73(1) (2012): 40-46.
- [54] Li, C., Feng, C., Peng, Z., Gong, W., and Kong, L. Ammonium-assisted green fabrication of graphene/natural rubber latex composite. Polymer Composites 34(1) (2013): 88-95.
- [55] Matos, C.F., Galembeck, F., and Zarbin, A.J.G. Multifunctional and environmentally friendly nanocomposites between natural rubber and graphene or graphene oxide. Carbon 78 (2014): 469-479.
- [56] Nakaramontri, Y., Kummerlowe, C., Nakason, C., and Vennemann, N. The effect of surface functionalization of carbon nanotubes on properties of natural rubber/carbon nanotube composites. Polymer Composites 36(11) (2015): 2113-2122.
- [57] Potts, J.R., Shankar, O., Du, L., and Ruoff, R.S. Processing-morphology-property relationships and composite theory analysis of reduced graphene

- oxide/natural rubber nanocomposites. Macromolecules 45(15) (2012): 6045-6055.
- [58] Potts, J.R., Shankar, O., Murali, S., Du, L., and Ruoff, R.S. Latex and two-roll mill processing of thermally-exfoliated graphite oxide/natural rubber nanocomposites. Composites Science and Technology 74 (2013): 166-172.
- [59] She, X., He, C., Peng, Z., and Kong, L. Molecular-level dispersion of graphene into epoxidized natural rubber: Morphology, interfacial interaction and mechanical reinforcement. Polymer 55(26) (2014): 6803-6810.
- [60] Sikong, L., Kooptarnond, K., Khangkhamano, M., and Sangchay, W. Superior properties of natural rubber enhanced by multiwall-carbon nanotubes/nanclay hybrid. Digest Journal of Nanomaterials and Biostructures 10(3) (2015): 1067-1110.
- [61] Stanier, D.C., Patil, A.J., Sriwong, C., Rahatekar, S.S., and Ciambella, J. The reinforcement effect of exfoliated graphene oxide nanoplatelets on the mechanical and viscoelastic properties of natural rubber. Composites Science and Technology 95 (2014): 59-66.
- [62] Sui, G., Zhong, W.H., Yang, X.P., and Yu, Y.H. Curing kinetics and mechanical behavior of natural rubber reinforced with pretreated carbon nanotubes. Materials Science and Engineering A 485(1-2) (2008): 524-531.



- [63] Sui, G., Zhong, W.H., Yang, X.P., and Zhao, S.H. Processing and material characteristics of a carbon-nanotube-reinforced natural rubber. Macromolecular Materials and Engineering 292(9) (2007): 1020-1026.
- [64] Tang, Z.H., Guo, B.C., Zhang, L.Q., and Jia, D.M. Graphene/Rubber Nanocomposites. Acta Polymerica Sinica (7) (2014): 865-877.
- [65] Wu, J., Xing, W., Huang, G., Li, H., Tang, M., Wu, S., and Lui, Y. Vulcanization kinetics of graphene/natural rubber nanocomposites. Polymer 54(13) (2013): 3314-3323.
- [66] Wu, L., Qu, P., Zhou, R., Wang, B., and Liao, S. Green synthesis of reduced graphene oxide and its reinforcing effect on natural rubber composites. High Performance Polymers 27(4) (2015): 486-496.
- [67] Wu, X., Lin, T.F., Tang, Z.H., Guo, B.C., and Huang, G.S. Natural rubber/graphene oxide composites: Effect of sheet size on mechanical properties and strain-induced crystallization behavior. Express Polymer Letters 9(8) (2015): 672-685.
- [68] Xing, W., Wu, J., Huang, G., Li, H., Tang, M., and Fu, X. Enhanced mechanical properties of graphene/natural rubber nanocomposites at low content. Polymer International 63(9) (2014): 1674-1681.
- [69] Yan, N., Buonocore, G., Lavorgna, M., Kaciulis, S., Balijepalli, S.K., Zhan, Y., Xia, H., and Ambrosio, L. The role of reduced graphene oxide on chemical,

- mechanical and barrier properties of natural rubber composites. Composites Science and Technology 102(1) (2014): 74-81.
- [70] Yang, H., Liu, P., Zhang, T., Duan, Y., and Zhang, J. Fabrication of natural rubber nanocomposites with high graphene contents via vacuum-assisted self-assembly. Rsc Advances 4(53) (2014): 27687-27690.
- [71] Yaragalla, S., Meera, A.P., Kalarikkal, N., and Thomas, S. Chemistry associated with natural rubber-graphene nanocomposites and its effect on physical and structural properties. Industrial Crops and Products 74 (2015): 792-802.
- [72] Zhao, L., Sun, X., Liu, Q., Zhao, J., and Xing, W. Natural rubber/graphene oxide nanocomposites prepared by latex mixing. Journal of Macromolecular Science - Physics 54(5) (2015): 581-592.
- [73] Ozbas, B., O'Neill, C.D., Register, R.A., Aksay, I.A., Prud'Homme, R.K., and Adamson, D.H. Multifunctional elastomer nanocomposites with functionalized graphene single sheets. Journal of Polymer Science Part B: Polymer Physics 50(13) (2012): 910-916.
- [74] Abd Razak, J., Haji Ahmad, S., Ratnam, C.T., Mahamood, M.A., and Mohamad, N. Effects of poly(ethyleneimine) adsorption on graphene nanoplatelets to the properties of NR/EPDM rubber blend nanocomposites. Journal of Materials Science 50(19) (2015): 6365-6381.
- [75] Aguilar-Bolados, H., Yazdani-Pedram, M., Brasero, J., and Lopez-Manchado, M.A. Influence of the Surfactant Nature on the Occurrence of Self-Assembly

- between Rubber Particles and Thermally Reduced Graphite Oxide during the Preparation of Natural Rubber Nanocomposites. Journal of Nanomaterials (2015): 7.
- [76] Lonkar, S.P., Deshmukh, Y.S., and Abdala, A.A. Recent advances in chemical modifications of graphene. Nano Research 8(4) (2015): 1039-1074.
- [77] Liu, L.H., Lerner, M.M., and Yan, M.D. Derivatization of Pristine Graphene with Well-Defined Chemical Functionalities. Nano Letters 10(9) (2010): 3754-3756.
- [78] Quintana, M., Spyrou, K., Grzelczak, M., Browne, W.R., Rudolf, P., and Prato, M. Functionalization of Graphene via 1,3-Dipolar Cycloaddition. Acs Nano 4(6) (2010): 3527-3533.
- [79] Seo, J.M. and Baek, J.B. A solvent-free Diels-Alder reaction of graphite into functionalized graphene nanosheets. Chemical Communications 50(93) (2014): 14651-14653.
- [80] Zhang, X.Y., Hou, L.L., Cossen, A., Coleman, A.C., Lvashenko, O., Rudolf, P., Vanwee, B.J., Browne, W.R., and Feringa, B.L. One-Pot Functionalization of Graphene with Porphyrin through Cycloaddition Reactions. Chemistry-a European Journal 17(32) (2011): 8957-8964.
- [81] Chidawanyika, W. and Nyokong, T. Characterization of amine-functionalized single-walled carbon nanotube-low symmetry phthalocyanine conjugates. Carbon 48(10) (2010): 2831-2838.

- [82] Ellison, M.D. and Gasda, P.J. Functionalization of single-walled carbon nanotubes with 1,4-benzenediamine using a diazonium reaction. Journal of Physical Chemistry C 112(3) (2008): 738-740.
- [83] De Falco, A., Marzocca, A.J., Corcuera, M.A., Eceiza, A., Momdragon, I., Rubiolo, G.H., and Goyanes, S. Accelerator Adsorption onto Carbon Nanotubes Surface Affects the Vulcanization Process of Styrene-Butadiene Rubber Composites. Journal of Applied Polymer Science 113(5) (2009): 2851-2857.
- [84] Zhang, B.L., Wang, Y.Z., Wang, P.Y., and Huang, H.H. Study on vulcanization kinetics of constant viscosity natural rubber by using a rheometer MDR2000. Journal of Applied Polymer Science 130(1) (2012): 47-53.
- [85] Wang, P.Y., Qinn, H.L., and Yu, H.P. Kinetics of natural rubber vulcanization in the end stage of curing period. Journal of Applied Polymer Science 101(1) (2006): 580-583.
- [86] Hertz Jr, D.L. Theory & practice of vulcanization. Elastomerics 116(11) (1984): 17-21.
- [87] Ding, R. and Leonov, A.I. A kinetic model for sulfur accelerated vulcanization of a natural rubber compound. Journal of Applied Polymer Science 61(3) (1996): 455-463.
- [88] Arrillaga, A., Zaldua, A.M., Atxurra, R.M., and Farid, A.S. Techniques used for determining cure kinetics of rubber compounds. European Polymer Journal 43(11) (2007): 4783-4799.

- [89] Su, C.C., Wei, C.H., and Li, B.C. Thermal and cure kinetics of epoxy molding compounds cured with thermal latency accelerators. Advances in Materials Science and Engineering 2013(391267) (2013): 1-9.
- [90] Vyazovkin, S., Burnham, A.K., Criado, J.M., Pérez-Maqueda, L.A., Popescu, C., and Sbirrazzuoli, N. ICTAC Kinetics committee recommendations for performing kinetic computations on thermal analysis data. Thermochimica Acta 520(1-2) (2011): 1-19.
- [91] Janković, B., Stopić, S., Güven, A., and Friedrich, B. Kinetic analysis of isothermal decomposition process of zinc leach residue in an inert atmosphere. the estimation of the apparent activation energy distribution. Mineral Processing and Extractive Metallurgy Review 35(4) (2014): 239-256.
- [92] Pinsanor, V., Junpoonsup, S., Patcharaphun, S., and Sombatsompop, N. Effects of Silica, Calcium Carbonate, and SiO<sub>2</sub>/CaCO<sub>3</sub> Blends on Properties of Cellular NR Compounds. in Proceedings of 41st Kasetsart University Annual Conference, pp. 517-524, 2003.
- [93] Ariff, Z.M., Zakaria, Z., Tay, L.H., and Lee, S.Y. Effect of foaming temperature and rubber grades on properties of natural rubber foams. Journal of Applied Polymer Science 107(4) (2008): 2531-2538.
- [94] Bokobza, L. and Rapoport, O. Reinforcement of natural rubber. Journal of Applied Polymer Science 85(11) (2002): 2301-2316.

- [95] Šesták, J., Kozmidis-Petrović, A., and Živković, Ž. Crystallization kinetics accountability and the correspondingly developed glass-forming criteria - A personal recollection at the forty years anniversaries. Journal of Mining and Metallurgy, Section B: Metallurgy 47(2) (2011): 229-239.
- [96] Sestak, J. Science of heat and thermophysical studies: a generalized approach to thermal analysis. Amsterdam: Elsevier Science, 2005.
- [97] Rodgers, B. and Waddell, W. Chapter 9 - The Science of Rubber Compounding. in Mark, J.E., Erman, B., and Roland, C.M. (eds.), The Science and Technology of Rubber (Fourth Edition), pp. 417-471. Boston: Academic Press, 2013.
- [98] Bruice, P.Y. Organic Chemistry. Fourth ed. New Jersey: Prentice Hall, 2004.
- [99] Carey, F.A. Organic Chemistry. Seventh ed. New York: The McGraw-Hill companies, Inc., 2008.
- [100] Hinds, W.C. Aerosol technology : properties, behavior and measurement of airborne particles. Second ed. New York: John Wiley & Sons, Inc, 1999.
- [101] Chien, S.K., Yang, Y.T., and Chen, C.K. Influence of chemisorption on the thermal conductivity of graphene nanoribbons. Carbon 50(2) (2012): 421-428.
- [102] Zhang, Y.Y., Pei, Q.X., He, X.Q., and Mai, Y.W. A molecular dynamics simulation study on thermal conductivity of functionalized bilayer graphene sheet. Chemical Physics Letters 622 (2015): 104-108.

- [103] Zhao, W.W., Wang, Y.L., Wu, Z.T., Wang, W.H., Bi, K.D., Liang, Z., Yang, J.K., Chen, Y.F., Xu, Z.P., and Ni, Z.H. Defect-Engineered Heat Transport in Graphene: A Route to High Efficient Thermal Rectification. Scientific Reports 5 (2015): 1-11.





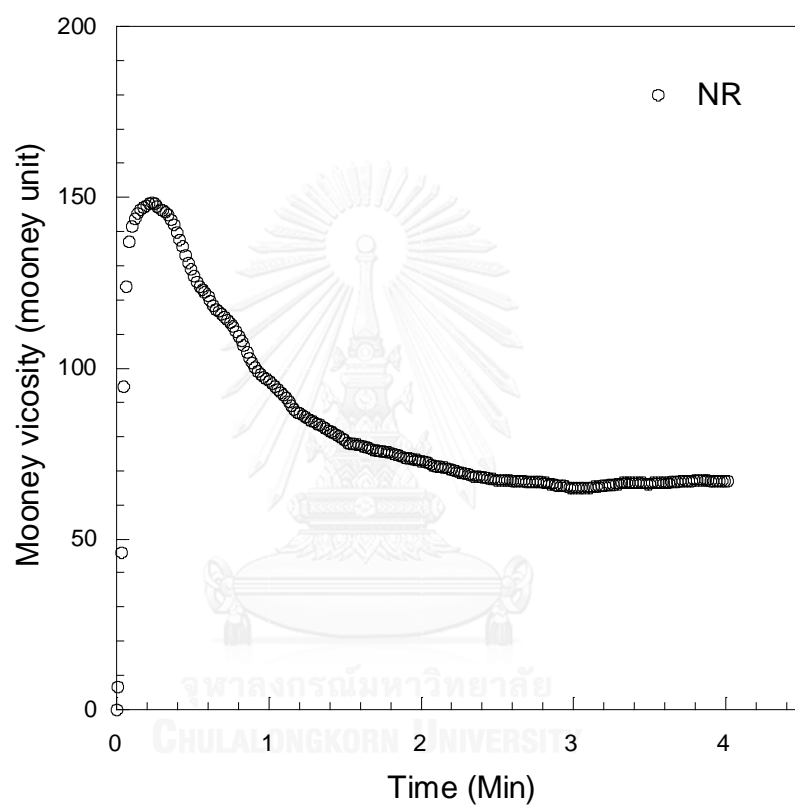
APPENDIX

จุฬาลงกรณ์มหาวิทยาลัย  
CHULALONGKORN UNIVERSITY



## Appendix A

## Mooney viscosity of natural rubber



## Appendix B

## Solvent absorption and gel content of vulcanized natural rubber

Sample Name	VNR before swelling (g)	VNR after swelling (g)	VNR after drying (g)	Solvent absorption (wt%)	Gel content (wt%)
VNR-MBS cure at 15 min	1.67±0.10	14.98±1.50	0.88±0.04	1609.93±102.23	52.55±1.16
VNR-MBS cure at 20 min	1.65±0.04	9.48±0.42	1.20±0.01	692.80±30.22	72.49±1.30
VNR-MBS cure at 25 min	1.65±0.02	8.68±0.05	1.29±0.01	572.48±3.84	78.00±0.86
VNR-MBS cure at 30 min	1.66±0.02	8.54±0.05	1.39±0.02	516.35±13.01	83.68±0.17

## Appendix C

## Particle size distribution

Table C1 Size distribution of NRF-MBS-B4

$D_{upper}$	$D_{lower}$	$\Delta D_i$	$D_i$	$n_i$	$f_{n_i}$	$f_{n_i}/DD_i$	$C_{n_i}$	$f_{n_i}D_i$	$D_i - D_a$	$(D_i - D_a)^2$	$f(D_i - D_a)^2$
120	130	10	125	7	0.044	0.004	0.044	5.469	-47.688	2274.098	99.492
130	140	10	135	15	0.094	0.009	0.138	12.656	-37.688	1420.348	133.158
140	150	10	145	19	0.119	0.012	0.256	17.219	-27.688	766.598	91.033
150	160	10	155	22	0.138	0.014	0.394	21.313	-17.688	312.848	43.017
160	170	10	165	23	0.144	0.014	0.538	23.719	-7.688	59.098	8.495
170	180	10	175	18	0.113	0.011	0.650	19.688	2.313	5.348	0.602
180	190	10	185	16	0.100	0.010	0.750	18.500	12.313	151.598	15.160
190	200	10	195	8	0.050	0.005	0.800	9.750	22.313	497.848	24.892
200	210	10	205	11	0.069	0.007	0.869	14.094	32.313	1044.098	71.782
210	220	10	215	4	0.025	0.003	0.894	5.375	42.313	1790.348	44.759
220	230	10	225	6	0.038	0.004	0.931	8.438	52.313	2736.598	102.622
230	240	10	235	6	0.038	0.004	0.969	8.813	62.313	3882.848	145.607
240	250	10	245	5	0.031	0.003	1.000	7.656	72.313	5229.098	163.409
				160	1			172.69			944.027

$$SD = \sqrt{\frac{\sum f(D_i - D_a)^2}{N}} = \sqrt{\frac{944.027}{160}} = 2.429$$

CHULALONGKORN UNIVERSITY

Table C2 Size distribution of NRF-TBS-B4

$D_{upper}$	$D_{lower}$	$\Delta Di$	$Di$	$ni$	$fni$	$fni/DDi$	$Cni$	$fniDi$	$Di-Da$	$(Di-Da)^2$	$f(Di-Da)^2$
120	130	10	125	12	0.075	0.008	0.075	9.375	-42.3	1785.063	133.880
130	140	10	135	22	0.138	0.014	0.213	18.563	-32.3	1040.063	143.009
140	150	10	145	23	0.144	0.014	0.356	20.844	-22.3	495.063	71.165
150	160	10	155	19	0.119	0.012	0.475	18.406	-12.3	150.063	17.820
160	170	10	165	18	0.113	0.011	0.588	18.563	-2.25	5.063	0.570
170	180	10	175	19	0.119	0.012	0.706	20.781	7.75	60.063	7.132
180	190	10	185	10	0.063	0.006	0.769	11.563	17.75	315.063	19.691
190	200	10	195	10	0.063	0.006	0.831	12.188	27.75	770.063	48.129
200	210	10	205	8	0.050	0.005	0.881	10.250	37.75	1425.063	71.253
210	220	10	215	7	0.044	0.004	0.925	9.406	47.75	2280.063	99.753
220	230	10	225	6	0.038	0.004	0.963	8.438	57.75	3335.063	125.065
230	240	10	235	5	0.031	0.003	0.994	7.344	67.75	4590.063	143.439
240	250	10	245	1	0.006	0.001	1.000	1.531	77.75	6045.063	37.782
				160	1			167.25			918.688

$$SD = \sqrt{\frac{\sum f(Di-Da)^2}{N}} = \sqrt{\frac{918.688}{160}} = 2.396$$

Table C3 Size distribution of NRF-CBS-B4

D <sub>uper</sub>	D <sub>lower</sub>	ΔDi	Di	ni	fni	fni/DDi	Cni	fniDi	Di-Da	(Di-Da) <sup>2</sup>	f(Di-Da) <sup>2</sup>
120	130	10	125	11	0.069	0.007	0.069	8.594	-39.938	1595.004	109.657
130	140	10	135	21	0.131	0.013	0.200	17.719	-29.938	896.254	117.633
140	150	10	145	23	0.144	0.014	0.344	20.844	-19.938	397.504	57.141
150	160	10	155	24	0.150	0.015	0.494	23.250	-9.938	98.754	14.813
160	170	10	165	19	0.119	0.012	0.613	19.594	0.063	0.004	0.000
170	180	10	175	16	0.100	0.010	0.713	17.500	10.063	101.254	10.125
180	190	10	185	14	0.088	0.009	0.800	16.188	20.063	402.504	35.219
190	200	10	195	11	0.069	0.007	0.869	13.406	30.063	903.754	62.133
200	210	10	205	11	0.069	0.007	0.938	14.094	40.063	1605.004	110.344
210	220	10	215	6	0.038	0.004	0.975	8.063	50.063	2506.254	93.985
220	230	10	225	3	0.019	0.002	0.994	4.219	60.063	3607.504	67.641
230	240	10	235	1	0.006	0.001	1.000	1.469	70.063	4908.754	30.680
				160	1			164.94		17022.547	709.371

$$SD = \sqrt{\frac{\sum f(Di-Da)^2}{N}} = \sqrt{\frac{709.371}{160}} = 2.105$$

Table C4 Size distribution of NRF-CBS2-B4

$D_{upper}$	$D_{lower}$	$\Delta Di$	$Di$	$ni$	$fni$	$fni/DDi$	$Cni$	$fniDi$	$Di-Da$	$(Di-Da)^2$	$f(Di-Da)^2$
120	130	10	125	14	0.088	0.009	0.088	10.938	-40.375	1630.141	142.637
130	140	10	135	16	0.100	0.010	0.188	13.500	-30.375	922.641	92.264
140	150	10	145	18	0.113	0.011	0.300	16.313	-20.375	415.141	46.703
150	160	10	155	25	0.156	0.016	0.456	24.219	-10.375	107.641	16.819
160	170	10	165	26	0.163	0.016	0.619	26.813	-0.375	0.141	0.023
170	180	10	175	17	0.106	0.011	0.725	18.594	9.625	92.641	9.843
180	190	10	185	13	0.081	0.008	0.806	15.031	19.625	385.141	31.293
190	200	10	195	13	0.081	0.008	0.888	15.844	29.625	877.641	71.308
200	210	10	205	10	0.063	0.006	0.950	12.813	39.625	1570.141	98.134
210	220	10	215	3	0.019	0.002	0.969	4.031	49.625	2462.641	46.175
220	230	10	225	2	0.013	0.001	0.981	2.813	59.625	3555.141	44.439
230	240	10	235	2	0.013	0.001	0.994	2.938	69.625	4847.641	60.596
240	250	10	245	1	0.006	0.001	1.000	1.531	79.625	6340.141	39.626
				160	1			165.38		23206.828	699.859

$$SD = \sqrt{\frac{\sum f(Di-Da)^2}{N}} = \sqrt{\frac{699.859}{160}} = 2.091$$

Table C5 Size distribution of NRF-CBS-B5

$D_{upper}$	$D_{lower}$	$\Delta D_i$	$D_i$	$n_i$	$f_{n_i}$	$f_{n_i}/DD_i$	$C_{n_i}$	$f_{n_i}D_i$	$D_i - D_a$	$(D_i - D_a)^2$	$f(D_i - D_a)^2$
180	190	10	185	12	0.052	0.005	0.052	9.652	-67.217	4518.178	235.731
190	200	10	195	10	0.043	0.004	0.096	8.478	-57.217	3273.830	142.340
200	210	10	205	12	0.052	0.005	0.148	10.696	-47.217	2229.482	116.321
210	220	10	215	15	0.065	0.007	0.213	14.022	-37.217	1385.134	90.335
220	230	10	225	30	0.130	0.013	0.343	29.348	-27.217	740.786	96.624
230	240	10	235	27	0.117	0.012	0.461	27.587	-17.217	296.439	34.799
240	250	10	245	21	0.091	0.009	0.552	22.370	-7.217	52.091	4.756
250	260	10	255	15	0.065	0.007	0.617	16.630	2.783	7.743	0.505
260	270	10	265	20	0.087	0.009	0.704	23.043	12.783	163.395	14.208
270	280	10	275	12	0.052	0.005	0.757	14.348	22.783	519.047	27.081
280	290	10	285	9	0.039	0.004	0.796	11.152	32.783	1074.699	42.053
290	300	10	295	13	0.057	0.006	0.852	16.674	42.783	1830.352	103.455
300	310	10	305	11	0.048	0.005	0.900	14.587	52.783	2786.004	133.244
310	320	10	315	3	0.013	0.001	0.913	4.109	62.783	3941.656	51.413
320	330	10	325	6	0.026	0.003	0.939	8.478	72.783	5297.308	138.191
330	340	10	335	4	0.017	0.002	0.957	5.826	82.783	6852.960	119.182
340	350	10	345	5	0.022	0.002	0.978	7.500	92.783	8608.612	187.144
350	360	10	355	5	0.022	0.002	1.000	7.717	102.783	10564.265	229.658
				230	1			252.22			1767.040

$$SD = \sqrt{\frac{\sum f(D_i - D_a)^2}{N}} = \sqrt{\frac{1767.04}{230}} = 2.772$$

Table C6 Size distribution of NRF-CBS-B5-UG1

D <sub>upper</sub>	D <sub>lower</sub>	ΔDi	Di	ni	fni	fni/DDi	Cni	fniDi	Di-Da	(Di-Da) <sup>2</sup>	f(Di-Da) <sup>2</sup>
140	150	10	145	13	0.057	0.006	0.057	8.196	-51.043	2605.437	147.264
150	160	10	155	15	0.065	0.007	0.122	10.109	-41.043	1684.567	109.863
160	170	10	165	24	0.104	0.010	0.226	17.217	-31.043	963.698	100.560
170	180	10	175	28	0.122	0.012	0.348	21.304	-21.043	442.828	53.909
180	190	10	185	30	0.130	0.013	0.478	24.130	-11.043	121.958	15.908
190	200	10	195	29	0.126	0.013	0.604	24.587	-1.043	1.089	0.137
200	210	10	205	27	0.117	0.012	0.722	24.065	8.957	80.219	9.417
210	220	10	215	17	0.074	0.007	0.796	15.891	18.957	359.350	26.561
220	230	10	225	11	0.048	0.005	0.843	10.761	28.957	838.480	40.101
230	240	10	235	4	0.017	0.002	0.861	4.087	38.957	1517.611	26.393
240	250	10	245	13	0.057	0.006	0.917	13.848	48.957	2396.741	135.468
250	260	10	255	7	0.030	0.003	0.948	7.761	58.957	3475.871	105.787
260	270	10	265	6	0.026	0.003	0.974	6.913	68.957	4755.002	124.044
270	280	10	275	6	0.026	0.003	1.000	7.174	78.957	6234.132	162.630
				230	1			196.04			1058.042

$$SD = \sqrt{\frac{\sum f(Di-Da)^2}{N}} = \sqrt{\frac{1058.042}{230}} = 2.145$$



Table C7 Size distribution of NRF-CBS-B5-UG2

D <sub>uper</sub>	D <sub>lower</sub>	ΔDi	Di	ni	fni	fni/DDi	Cni	fniDi	Di-Da	(Di-Da) <sup>2</sup>	f(Di-Da) <sup>2</sup>
150	160	10	155	8	0.035	0.003	0.035	5.391	-47.087	2217.181	77.119
160	170	10	165	22	0.096	0.010	0.130	15.783	-37.087	1375.442	131.564
170	180	10	175	23	0.100	0.010	0.230	17.500	-27.087	733.703	73.370
180	190	10	185	24	0.104	0.010	0.335	19.304	-17.087	291.964	30.466
190	200	10	195	25	0.109	0.011	0.443	21.196	-7.087	50.225	5.459
200	210	10	205	31	0.135	0.013	0.578	27.630	2.913	8.486	1.144
210	220	10	215	40	0.174	0.017	0.752	37.391	12.913	166.747	28.999
220	230	10	225	25	0.109	0.011	0.861	24.457	22.913	525.008	57.066
230	240	10	235	15	0.065	0.007	0.926	15.326	32.913	1083.268	70.648
240	250	10	245	17	0.074	0.007	1.000	18.109	42.913	1841.529	136.113
				230	1			202.09			611.949

$$SD = \sqrt{\frac{\sum f(Di-Da)^2}{N}} = \sqrt{\frac{611.949}{230}} = 1.631$$

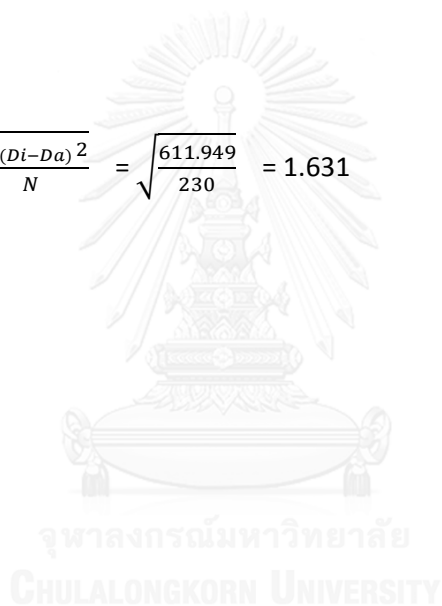


Table C8 Size distribution of NRF-CBS-B5-UG3

D <sub>uper</sub>	D <sub>lower</sub>	ΔDi	Di	ni	fni	fni/DDi	Cni	fniDi	Di-Da	(Di-Da) <sup>2</sup>	f(Di-Da) <sup>2</sup>
120	130	10	125	19	0.083	0.008	0.083	10.326	-37.565	1411.146	116.573
130	140	10	135	25	0.109	0.011	0.191	14.674	-27.565	759.841	82.591
140	150	10	145	37	0.161	0.016	0.352	23.326	-17.565	308.537	49.634
150	160	10	155	32	0.139	0.014	0.491	21.565	-7.565	57.233	7.963
160	170	10	165	31	0.135	0.013	0.626	22.239	2.435	5.928	0.799
170	180	10	175	25	0.109	0.011	0.735	19.022	12.435	154.624	16.807
180	190	10	185	21	0.091	0.009	0.826	16.891	22.435	503.319	45.955
190	200	10	195	26	0.113	0.011	0.939	22.043	32.435	1052.015	118.923
200	210	10	205	14	0.061	0.006	1.000	12.478	42.435	1800.711	109.608
				230		1		162.57			548.854

$$SD = \sqrt{\frac{\sum f(Di-Da)^2}{N}} = \sqrt{\frac{548.854}{230}} = 1.545$$

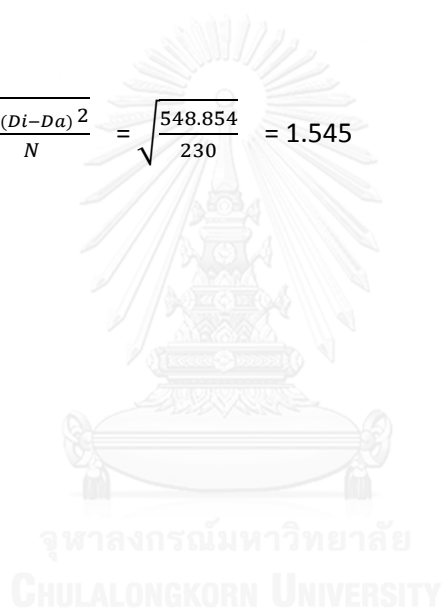
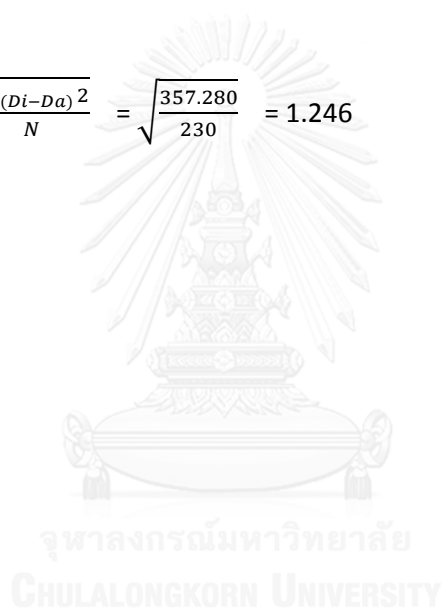


Table C9 Size distribution of NRF-CBS-B5-CG3

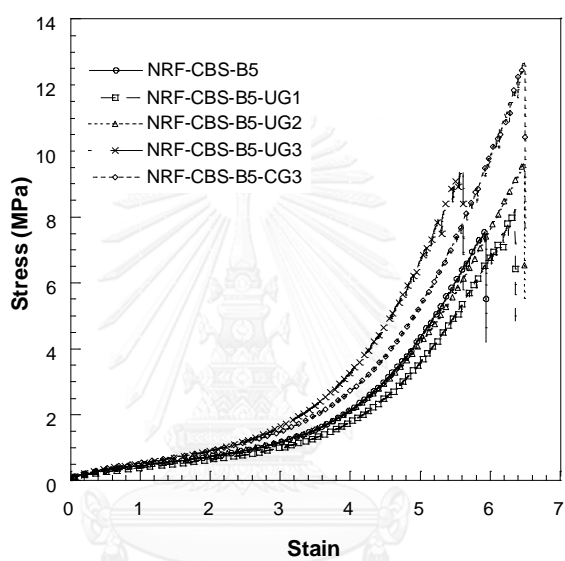
$D_{upper}$	$D_{lower}$	$\Delta Di$	$Di$	$ni$	$fni$	$fni/DDi$	$Cni$	$fniDi$	$Di-Da$	$(Di-Da)^2$	$f(Di-Da)^2$
130	140	10	135	5	0.022	0.002	0.022	2.935	-37.261	1388.372	30.182
140	150	10	145	30	0.130	0.013	0.152	18.913	-27.261	743.155	96.933
150	160	10	155	35	0.152	0.015	0.304	23.587	-17.261	297.938	45.338
160	170	10	165	35	0.152	0.015	0.457	25.109	-7.261	52.720	8.023
170	180	10	175	38	0.165	0.017	0.622	28.913	2.739	7.503	1.240
180	190	10	185	38	0.165	0.017	0.787	30.565	12.739	162.285	26.812
190	200	10	195	33	0.143	0.014	0.930	27.978	22.739	517.068	74.188
200	210	10	205	16	0.070	0.007	1.000	14.261	32.739	1071.851	74.564
				230	1			172.26			357.280

$$SD = \sqrt{\frac{\sum f(Di-Da)^2}{N}} = \sqrt{\frac{357.280}{230}} = 1.246$$



## Appendix D

Stress-stain curve of NR/graphene nanocomposite foam



## VITA

Mr. Pollawat Jaroenthonkajonchai was born in Chonburi, Thailand on April 8, 1985. He completed high school at Panuspittayakhan School, Thailand in 2004 and received Bachelor's Degree of Science from the Department of Chemical Technology, Faculty of Science, Chulalongkorn University, Thailand in 2008. He graduated Master's Degree in Chemical Engineering at the Department of Chemical Engineering, Faculty of Engineering, Chulalongkorn University on March, 2012. After that, he furthered his Doctoral Degree study in Chemical Engineering at the Department of Chemical Engineering, Faculty of Engineering, Chulalongkorn University on October, 2012. He received the Royal Golden Jubilee Ph.D. Scholarship (PHD/0264/2553) by Thailand Research Fund for his financial support during his Doctoral Degree.

In addition, he had a published article in Journal of cellular plastics. The publication entitled "Effect of azodicarbonamide on microstructure, cure kinetics and properties of natural rubber foam". He was invited for oral presentation on The 2nd Polymer Conference of Thailand (PCT-2). The title of this presentation was "Rheological properties of graphene suspension in poly [(phenyl glycidyl ether)-co-formaldehyde]". This conference was held during October 20-21, 2011 in Bangkok, Thailand. During his Doctoral degree study, he was invited for oral presentation on RGJ-Phd Congress XVI Conference in Thailand entitled "Influence of blowing agent content and sulfenamide accelerators on properties of natural rubber foam" and he also was invited for poster presentation on the International Rubber Conference 2016 entitled "Kinetic study of natural rubber foam product". The first conference was held during June 11-13, 2015 at Chonburi, Thailand. The second conference will hold on October 24-28, 2016 at Kitakyushu, Japan.